Initial ciliary assembly in *Chlamydomonas* requires Arp2/3 complex-dependent endocytosis

Brae M Bigge[1,2], Nicholas E Rosenthal[1,2], Prachee Avasthi[1,2]

[1]Biochemistry and Cell Biology Department, Geisel School of Medicine at Dartmouth College, Hanover, New Hampshire
[2]Anatomy and Cell Biology Department, University of Kansas Medical Center, Kansas City, Kansas

ABSTRACT

Ciliary assembly, trafficking, and regulation are dependent on microtubules, but the mechanisms of ciliary assembly also require the actin cytoskeleton. Here, we dissect subcellular roles of actin in ciliogenesis by focusing on actin networks nucleated by the Arp2/3 complex in the powerful ciliary model, *Chlamydomonas*. We find the Arp2/3 complex is required for the initial stages of ciliary assembly when protein and membrane are in high demand, but cannot yet be supplied from the Golgi complex. We provide evidence for Arp2/3 complex-dependent clathrin-mediated endocytosis of ciliary proteins, an increase in endocytic activity upon induction of ciliary growth, and relocalization of plasma membrane proteins to newly formed cilia. Our data support a new model of ciliary protein and membrane trafficking during early ciliogenesis whereby proteins previously targeted to the plasma membrane are reclaimed by Arp2/3 complex-dependent clathrin-mediated endocytosis for initial ciliary assembly.

INTRODUCTION

The cilium of the unicellular, green alga *Chlamydomonas reinhardtii* has long been used as a model due to its structural and mechanistic conservation relative to the cilia of mammalian cells. Cilia consist primarily of microtubules that extend from the surface of the cell and are ensheathed in plasma membrane. Their assembly relies on microtubule dynamics and trafficking of protein and membrane (Nachury, Seeley, and Jin 2010), as well as intraflagellar transport (IFT), a motor-based transport system that moves tubulin and other cargo from the base of the cilium to the tip and back again (Pedersen and Rosenbaum 2008).

Although cilia are composed of microtubules and depend on them for assembly, the mechanisms governing ciliary maintenance and assembly extend to other cytoskeletal components, namely actin. In fact, the microtubule organizing center of the cell, the centrosome, from which cilia are nucleated has been found to function as an actin organizer (Farina et al. 2016; Inoue et al. 2019). In mammalian cells, cortical actin disruption results in increased ciliary length and percentage of ciliated cells (Kim et al. 2010; Park et al. 2008). Further, in mammalian cells, when ciliogenesis is triggered by serum starvation, preciliary vesicles are trafficked to the centriole where they fuse to form a ciliary vesicle around the budding cilium. In the intracellular pathway of ciliogenesis, it has been shown that when Arp2/3 complex-branched actin is lost, depletion of preciliary vesicles at the centriole occurs due to problems with vesicle fusion, suggesting a role for branched actin in intracellular ciliogenesis (Wu, Chen, and Tang 2018). Further, actin itself has even been found within cilia, suggesting that actin is a key protein involved in ciliary maintenance and assembly (Kiesel et al. 2020).

Chlamydomonas cells are ideal for tackling the question of actin-dependent ciliary trafficking due to their lack of a cortical actin network and their ability to undergo consistent and robust ciliogenesis without requiring serum starvation. In *Chlamydomonas*, disruption of actin networks with Cytochalasin D (CytoD) resulted in shorter steady-state cilia (W. L. Dentler and Adams 1992) and disruption with Latrunculin B (LatB), which sequesters monomers leading to eventual filament depolymerization, resulted in shortened cilia and impaired regeneration (Avasthi et al. 2014; Jack et al. 2019). *Chlamydomonas* actin networks are required for accumulation of IFT machinery at the base of cilia and for entry of IFT material into cilia (Avasthi et al. 2014), as well as for trafficking of post-Golgi vesicles to cilia, the synthesis of ciliary proteins, and the organization of the gating region at the base of cilia (Jack et al. 2019). Many key advances in our understanding of the relationship between cilia and actin have been discovered using *Chlamydomonas*, which is proving to be a useful model for studying the actin cytoskeleton and its ciliary functions.

The actin cytoskeleton of *Chlamydomonas* contains two actin genes: *IDA5*, a conventional actin with 91% sequence identity to human β-actin; and *NAP1*, a divergent actin that shares only 63% of its sequence with human β-actin (Hirono et al. 2003; Kato-Minoura et al. 1998). We consider NAP1 to be an actin-like protein as opposed to an actin related protein (ARP) because it has a higher sequency identity to actin than to conventional ARPs, and because it is able to functionally compensate for the conventional filamentous actin (Jack et al. 2019; M. Onishi et al. 2018; M. Onishi, Pringle, and Cross 2016; Masayuki Onishi et al. 2019). Under normal, vegetative conditions, the conventional IDA5 is the primary actin expressed, but when cells are treated with LatB, the LatB-insensitive NAP1 is upregulated (M. Onishi et al. 2018; M. Onishi, Pringle, and Cross 2016; Hirono et al. 2003). This separability of the two actins has led to the discovery that they can compensate for each other in ciliary maintenance and assembly (Jack et al. 2019). Studies of the role of actin in ciliary assembly have used global disruption by knocking out either one of the filamentous actins or acutely knocking out both, yet actin networks have diverse compositions and topologies that lead to specific subfunctions within cells.

Actin networks rely on the actin binding proteins that contribute to the formation, arrangement, and function of the network. One such actin binding protein is the Arp2/3 complex,

which nucleates branched or dendritic actin networks by nucleating a daughter filament off the side of an existing mother filament. The dendritic networks nucleated by the Arp2/3 complex are primarily found to be responsible for functions that involve membrane remodeling, for example lamellipodia and endocytosis (Campellone and Welch 2010). The Arp2/3 complex from most eukaryotes consists of seven subunits: Arp2, Arp3, and ARPC1-5 (**Supplemental Figure 1**) and each subunit plays a specific role of varying importance in the nucleation process. ARPC2 and ARPC4 form the core of the complex and the primary contacts with the mother filament, Arp2 and Arp3 serve as the first subunits of the daughter filament, and ARPC1 and ARPC3 play a role in nucleation but are not critical for branch formation (Robinson et al. 2001; Gournier et al. 2001). Each of these subunits are found in *Chlamydomonas* but have varying degrees of sequence homology compared with conventional Arp2/3 complexes (**Supplemental Figure 1**). Interestingly, the ARPC5 subunit has yet to be found in *Chlamydomonas*. ARPC5 is thought to be important for the association of ARPC1 to the complex, but a mammalian complex lacking ARPC5 and ARPC1 maintains some nucleating and branching activity and is able to cross-link actin normally (Gournier et al. 2001).

Here, using the chemical inhibitor CK-666 to inhibit the nucleating function of the Arp2/3 complex (Hetrick et al. 2013) and a genetic mutant of a critical Arp2/3 complex member, ARPC4 (Cheng et al. 2017; Li et al. 2019), we take a more delicate approach to investigating the role of actin in ciliary assembly by separating different actin networks into their subfunctions based on topology. Specifically, we probe the involvement of actin networks nucleated by the Arp2/3 complex in ciliary maintenance and assembly. This approach in these cells has allowed us to propose a new model implicating a subset of filamentous actin in redistribution of membrane and proteins for the initial stages of ciliogenesis.

RESULTS

Loss of Arp2/3 complex function inhibits normal regeneration and maintenance of cilia:

To answer questions involving the role of Arp2/3 complex-mediated actin networks in ciliary assembly, we primarily used two tools. First, we used the chemical inhibitor CK-666 which blocks the nucleating ability of the Arp2/3 complex. Second, we obtained a null mutant of the critical Arp2/3 complex member, ARPC4 (Cheng et al. 2017; Li et al. 2019) from the *Chlamydomonas* Resource Center. This *arpc4* mutant was confirmed via PCR (**Supplemental Figure 2A**). We further evaluated this mutant by creating a genetic rescue where a V5-tagged ARPC4 construct is expressed in *arpc4* mutant cells, *arpc4:*ARPC4-V5. This was confirmed via PCR, western blot, and immunofluorescence (**Supplemental Figure 2**).

We first investigated the requirement for the Arp2/3 complex in maintenance of cilia by treating cells with varying concentrations of CK-666 or the inactive control CK-689 (250μM) for 2 hours and measuring the effect on steady state ciliary length. Consistent with previous results (Avasthi et al. 2014), we found that treating cells with CK-666 decreased ciliary length, suggesting that the Arp2/3 complex is required for maintaining cilia (**Figure 1A**). We saw no changes in ciliary length with the inactive CK-689 (**Figure 1A**) or when *arpc4* mutant cells lacking a functional Arp2/3 complex were treated with CK-666 (**Supplemental Figure 3-4**). Untreated *arpc4* mutant cells did however recapitulate the CK-666 result by showing a decreased ciliary length when compared with wild-type cells (**Figure 1B**). This defect in ciliary length was not present in the rescue, *arpc4:*ARPC4-V5 (**Figure 1B**). Overall, these results demonstrate through both chemical and genetic perturbation that the Arp2/3 complex is required for normal ciliary length maintenance.

Next, we probed the involvement of Arp2/3 complex-nucleated actin in the more complicated process of ciliary assembly where there is a high demand for protein and membrane both from pools already existing in the cell and from synthesis (Wingfield et al. 2017;

126 Nachury, Seeley, and Jin 2010; Rohatgi and Snell 2010; Jack et al. 2019; Diener, Lupetti, and
127 Rosenbaum 2015). Cells were deciliated by low pH shock and then allowed to synchronously
128 regenerate cilia after being returned to normal pH (Paul A. Lefebvre 1995). We found that cells
129 lacking a functional Arp2/3 complex were slow to regenerate their cilia, and two-thirds of cells
130 did not regrow cilia at all (**Figure 1C**). This phenotype could be rescued by expression of
131 ARPC4-V5 in the *arpc4* mutant (**Figure 1D**). Importantly, the most severe defect in assembly
132 appeared to be in the initial steps when existing protein and membrane are being incorporated
133 into cilia.
134 The striking decrease in ciliary assembly is puzzling because the loss of Arp2/3 complex
135 function, and therefore only a subset of actin filaments, results in a more dramatic phenotype
136 than that of the *nap1* mutants treated with LatB, which are lacking all filamentous actins (Jack et
137 al. 2019). However, in the *arpc4* mutant cells, a functional Arp2/3 complex never exists, and
138 therefore, cells never have Arp2/3 complex-mediated actin networks. In *nap1* mutant cells
139 treated with LatB, the treatment begins shortly after deciliation resulting in an acute perturbation.
140 Further, LatB functions by sequestering actin monomers to promote filament disassembly, and
141 thus the effects may not be immediate (Spector et al. 1989). Therefore, it is likely that there is a
142 brief window where actin filaments can assert their initial role in ciliary regeneration before being
143 depolymerized. To avoid this, we began the LatB treatment in *nap1* mutants 30 minutes before
144 deciliation. This pre-treatment allows us to observe what happens when actin is not present
145 immediately after deciliation. (**Figure 1E-F**). In this case, we see slightly decreased ciliary length
146 consistent with the acute treatment but dramatically decreased percent ciliation, which is
147 consistent with the *arpc4* mutant results.
148 This can also be observed with the inhibitor of the Arp2/3 complex, CK-666. In cells
149 treated with CK-666 immediately following deciliation, there is likely a window where the Arp2/3
150 complex can assert its role in assembly before being inhibited by CK-666. By pre-treating cells
151 with CK-666 for 1 hour before deciliation, we are able to observe what happens in the absence
152 of Arp2/3 complex function immediately following deciliation. When we do so, we see a more
153 dramatic defect in both ciliary length and percent ciliation than we do with just acute CK-666
154 treatment (**Figure 1G-H**), suggesting that the Arp2/3 complex is required for some very early
155 initial step of ciliary assembly that occurs even before we have a chance to treat the cells.
156

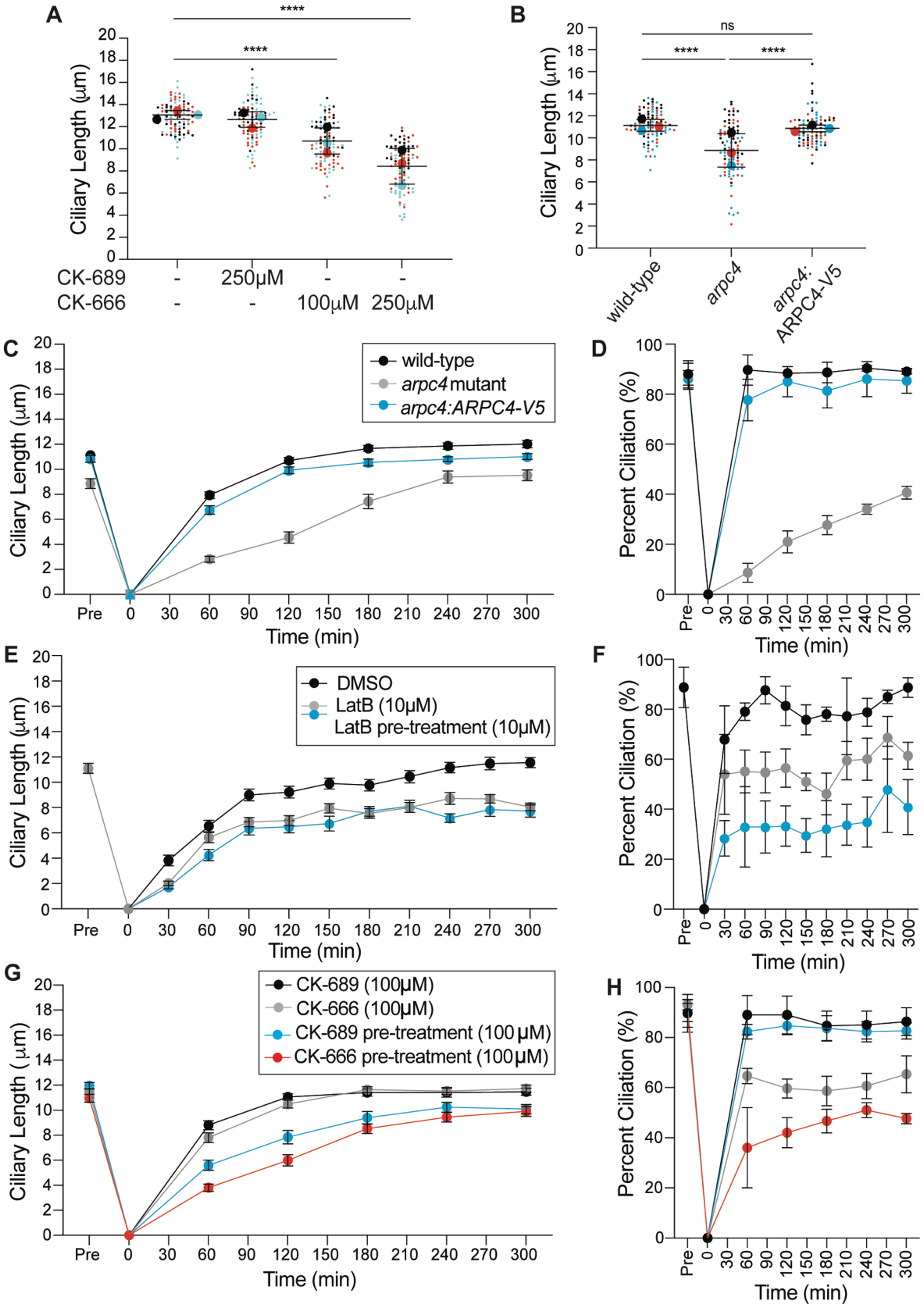

Figure 1. The Arp2/3 complex is required for normal ciliary maintenance and assembly. A) Wild-type cells containing a full active Arp2/3 complex were treated with 100µM or 250µM CK-666 or the inactive CK-689 for 2 hours.

Cells were then imaged using a DIC microscope and cilia were measure in ImageJ. Superplots are used to show the mean of 3 separate experiments with error bars representing standard deviation. n=30 for each treatment in 3 separate experiments. P<0.0001. **B)** Wild-type cells, *arpc4* mutant cells, and *arpc4* mutant cells expressing *ARPC4-V5* steady state cilia were also measured with no treatment. Superplots are used to show the mean of 3 separate experiments with error bars representing standard deviation. n=30 for each strain for 3 separate experiments. P<0.0001. **C)** Wild-type cells and *arpc4* mutant cells were deciliated using a pH shock and then cilia were allowed to regrow. The black line represents wild-type, while the grey line represents the *arpc4* mutant. The numbers above or below each point show the percent ciliation for the wild-type and *arpc4* mutant cells respectively. Means are displayed with error bars representing 95% confidence interval. n=30 for each strain and each time point in 3 separate experiments. For every time point except 0 min, P<0.0001 in terms of both length and percent ciliation. **D)** Wild-type cells, *arpc4* mutant cells, and *arpc4* mutant cells expressing *ARPC4-V5* were deciliated using a pH shock and then allowed to regrow. The black line represents wild-type, while the grey line represents the *arpc4* mutant and the cyan line represent the *arpc4* mutant expressing *ARPC4-V5*. Means are displayed with error bars representing 95% confidence interval. n=30 for each strain and each time point in 3 separate experiments. **E)** *nap1* mutant cells were pre-treated with 10μM LatB for 30 minutes before deciliation or treated with LatB upon the return to neutral pH following deciliation. The black line represents untreated cells, while the light grey line represents cells treated with LatB following deciliation and the dark grey line represents cells pre-treated with LatB. Error bars represent 95% confidence interval. n=30 for 3 separate experiments. For every time point P>0.0001 between DMSO and treated samples, except 30min (10μM LatB) which is ns. **F)** Percent ciliation for the experiment in D. Line color is the same as D. Error bars represent standard deviation. **G)** Wild-type cells were pre-treated with CK-666 or the inactive CK-689 (100μM) for 1 hour befoe deciliation of treated with CK-666 or the inactive CK-689 (100μM) following deciliation. Error bars represent 95% confidence interval. n=30 for 3 separate experiments. **H)** Percent ciliation for the experiments in G. Error bars represent standard deviation. n=100 in 3 separate experiments.

The Arp2/3 complex is required for the incorporation of existing membrane and proteins for ciliary assembly:

There are several distinct, filamentous actin-dependent steps of ciliary assembly after severing, including the incorporation of existing protein and membrane and the synthesis of new protein for cilia. Using a method that labels nascent peptides, we found that loss of ARPC4 did not prevent upregulation of translation following deciliation (**Supplemental Figure 5**). In this experiment, we are halting translation and fluorescently labelling newly translated polypeptides. Wild-type and *arpc4* mutant cells were tested using this reaction either before deciliation, following deciliation and one hour of regrowth, or following deciliation and one hour of regrowth in cycloheximide (CHX), which blocks protein synthesis by blocking the elongation step of protein translation. Both wild-type and *arpc4* mutant cells displayed an increase in cell fluorescence, especially in the area around the nucleus, following deciliation, indicating an increase in protein synthesis following deciliation (**Supplemental Figure 5**). Importantly, this increase in cell fluorescence was not significantly different between wild-type and *arpc4* mutant cells, suggesting that the loss of Arp2/3 complex function does not prevent the upregulation of protein synthesis that follows deciliation. This also suggests that the cells are aware that the cilia have been severed, as they respond with increased protein synthesis.

Given that *arpc4* mutant cells respond to deciliation with protein synthesis, another possibility for the role of the Arp2/3 complex in ciliary assembly involves the first step, which requires that a pool of existing proteins and membrane are incorporated into cilia in an actin-dependent manner (Jack et al. 2019). Further, disruption of Arp2/3 complex-mediated actin networks results in slow initial ciliary assembly, when it is likely that existing protein is being incorporated. We tested this by treating cells with cycloheximide (CHX), a protein synthesis inhibitor, we can eliminate the contribution of two steps in the process of ciliary assembly (**Figure 2A, Supplemental Figure 4**) (Rosenbaum, Moulder, and Ringo 1969). Without protein synthesis, there is no trafficking or incorporation of new proteins. Therefore, any ciliary growth we see is due to the incorporation of the existing protein alone. Under normal conditions, cells that are deciliated and treated with cycloheximide typically grow cilia to about half-length, or 6μm, within 2 hours (**Figure 2B**). In the *arpc4* mutant strain treated with CK-666, cilia display minimal growth (**Figure 2B**). In fact, throughout a five-hour period, only 6% of cells were able to

form cilia at all (**Figure 2B**). This suggests that the Arp2/3 complex and the actin networks nucleated by the complex are indispensable for the incorporation of existing protein and membrane during ciliary assembly.

We suspected that the *arpc4* mutant cells either lacked the normal pool of ciliary precursor proteins or were unable to incorporate it. However, the inability of the genetic mutants to regenerate in cycloheximide prevents us from being able to do the typical studies testing new protein synthesis, precursor pool size, and new protein incorporation outlined in Jack et al. 2018 as they all require regeneration in cycloheximide. To get around this, we used an acute perturbation through chemical inhibition in wild-type cells that have a normal ciliary precursor pool (as evidenced by their ability to grow to half-length in cycloheximide). These cells were deciliated and then CK-666 was added (in addition to cycloheximide) only for the regrowth, and thus it was not able to affect the size of the precursor pool. Cells treated with CK-666 and cycloheximide could not incorporate the precursor pool we know exists in these wild-type cells into cilia, while cilia of cells treated with only cycloheximide or cycloheximide and the inactive control for CK-666, CK-689 were able to grow to half length (**Figure 2C-D, Supplemental Figure 4**). This suggests that the problem with incorporation we see in cells lacking a functional Arp2/3 complex lies outside of the availability of the precursor pool.

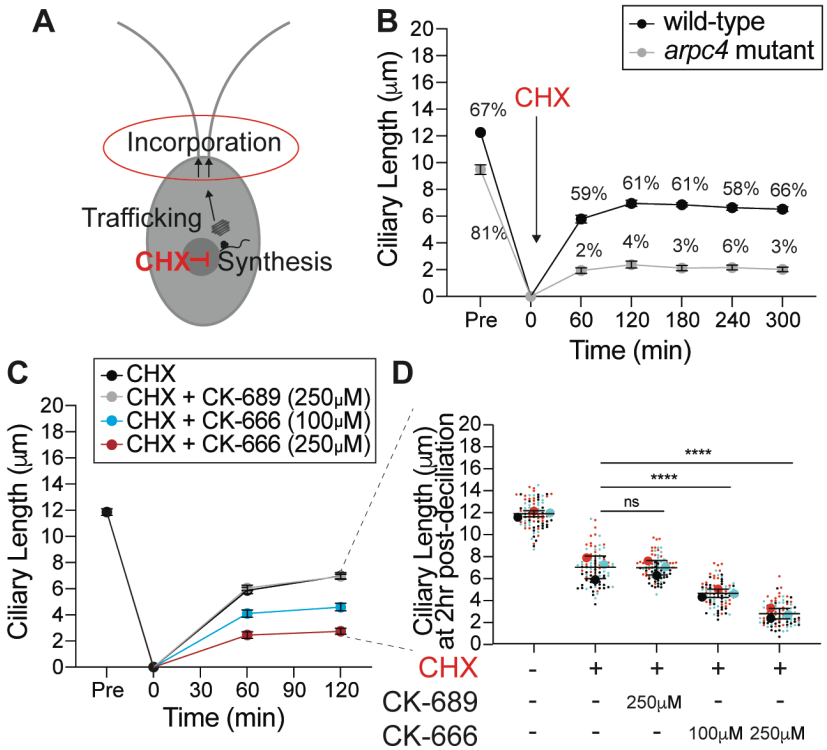

Figure 2. The Arp2/3 complex is required for incorporation of existing protein during ciliary assembly. A) Treating cells with cycloheximide inhibits protein synthesis, which means only incorporation of existing protein into the cilia is observed**. B)** Wild-type cells and *arpc4* mutants were deciliated and then allowed to regrow in 10μM CHX. The percentages above the lines represent the percent of cells with cilia at the indicated time points. The mean is shown with error bars representing 95% confidence interval. n=30 for each strain and each time point in 3 separate experiments. For every time point besides 0 min, P<0.0001 for both length and percent ciliation. **C)** Wild-type cells were deciliated and then treated with a combination of 10μM cycloheximide (CHX) and CK-666 (100μM or 250μM) or CK-689 (the inactive control, 250μM) at the same concentration during regrowth. The mean is shown with error bars representing 95% confidence interval. n=30 for each strain and each time point in 3 separate experiments. At both 1 and 2 hour time points P<0.0001 for cells treated with CK-666 compared to wild-type cells, and ns for cells treated with CK-689 compared to wild-type cells. **D)** The graph shows the 2 hour time point from C, or the length of their cilia after 2 hours of treatment and regrowth. Superplots are used to show the mean of 3 separate experiments with error

bars representing standard deviation. n=30 for each treatment group 3 separate experiments. For both the 100μM and 250μM CK-666 treatments with CHX, P<0.0001.

Cilia of *arpc4* mutant cells resorb faster in the absence of the Golgi:

Because we see defects in ciliary assembly and maintenance when cells are likely incorporating existing protein, and we know the protein needed for assembly is in excess due to our acute perturbations with CK-666, we next investigated membrane delivery to cilia. This is of particular interest as the Arp2/3 complex is canonically thought to be involved in membrane remodeling functions. Typically, the Golgi is thought to be the main source of membrane for cilia (Nachury, Seeley, and Jin 2010; Rohatgi and Snell 2010), and both ciliary membrane, membrane proteins, and even axonemal proteins are transported in or attached to vesicles in cytosol (Wood and Rosenbaum 2014). In *Chlamydomonas*, this has been demonstrated by the ciliary shortening of cells treated with Brefeldin A (BFA), a drug that causes Golgi collapse by interfering with ER to Golgi transport (W. Dentler 2013). To determine if the Arp2/3 complex is involved in the trafficking of new protein from the Golgi to cilia, we examined the Golgi following deciliation using transmission electron microscopy (TEM) in *arpc4* mutants (**Supplemental Figure 6A**). The Golgi appeared grossly normal, and in all cases had approximately the same number of cisternae (**Supplemental Figure 6A-B**) and did not show an abnormal accumulation of post-Golgi membrane as previously reported when perturbing all filamentous actin (Jack et al., 2019).

Alternative pathways for delivery of material to the cilia have also been found in *Chlamydomonas*. For example, surface proteins were biotinylated and then cells were deciliated, meaning the membrane and proteins within cilia were lost. When cilia were allowed to regrow, biotinylated proteins were found to reside within the new cilia suggesting they came from the plasma membrane (W. Dentler 2013). Therefore, we hypothesized that due to its role in membrane remodeling, and particularly endocytosis, in other organisms, the Arp2/3 complex may be part of an endocytic pathway that provides membrane and perhaps membrane proteins to cilia (**Figure 3A**). To test if membrane could be coming from an endosomal or endocytic source other than the Golgi, we treated cells with 36μM BFA to collapse the Golgi and block exocytosis so cells would be forced to utilize other sources of ciliary proteins and membranes. Wild-type cilia treated with BFA resorb slowly, but *arpc4* mutant cells had a faster resorption rate (**Figure 3B and D, Supplemental Figure 4**). Further, the number of cells with cilia in the *arpc4* mutant cells dramatically decreased with BFA treatment (**Figure 3C**). Meanwhile, cells treated with other known ciliary resorption-inducing drugs that do not specifically target Golgi traffic, 3-isobutyl-1-methylxanthine (IBMX) (Pasquale and Goodenough 1987) or sodium pyrophosphate (NaPPi) (P. A. Lefebvre et al. 1978) show an increased velocity of resorption in the wild-type cells compared to the *arpc4* mutant cells (**Supplemental Figure 7**), suggesting the faster resorption of the *arpc4* mutant cells in BFA is specific to the effects of BFA on the cell. Thus, wild-type cells are more capable of maintaining cilia without membrane supply from the Golgi, suggesting that there must be another source for membrane that is dependent upon the Arp2/3 complex.

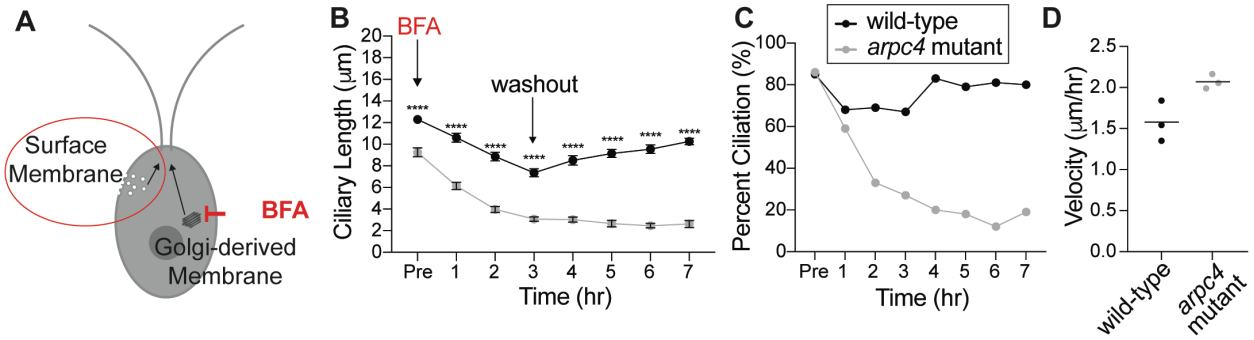

Figure 3. The Arp2/3 complex is required for ciliary maintenance in the absence of intact Golgi. A) Treating cells with Brefeldin A (BFA) causes the Golgi to collapse meaning any membranes and proteins used to maintain the cilia must come from other sources. **B)** Cells were treated with 36μM BFA for 3 hours at which time the drug was washed out. Wild-type is represented by black, while *arpc4* mutants are grey. The mean is shown with error bars representing 95% confidence interval. Error bars represent 95% confidence interval of the mean. n=30 for each time point and each strain in 3 separate experiments. **** represents P<0.0001. **C)** Percent ciliation of the cells in B. n=100. **D)** Resorption speed for wild-type cells and *arpc4* mutant cells as determined by fitting a line to the first 4 time points before washout and determining the slope of the line. Line represents the mean of 3 separate experiments. N=3. P=0.0314

Apical actin dots are dependent on the Arp2/3 complex:

Since ciliary membrane proteins can come from the Golgi or the plasma membrane and *arpc4* mutant cells have a more severe defect in incorporating ciliary proteins from non-Golgi sources, we asked if Arp2/3 complex-mediated actin networks might be responsible for endocytosis from the plasma membrane in *Chlamydomonas* as it is in other organisms. To determine where in the cell Arp2/3 complex-mediated actin networks might be acting, we looked directly at the effects of loss of Arp2/3 complex function on the actin structures in the cell. Using new protocols for the visualization of actin in *Chlamydomonas* developed by our lab (Craig et al. 2019), we stained wild-type cells and *arpc4* mutant cells with fluorescent phalloidin. In wild-type cells, apical dots reminiscent of endocytic actin patches in yeast are typically seen near the base of cilia (**Figure 4A**). We quantified the presence of these dots in the wild-type cells compared to the *arpc4* mutant cells (**Figure 4A-B**). We found that while about 70% of wild-type cells contain the dots, only about 5% of the *arpc4* mutant cells had dots (**Figure 4B**), suggesting the Arp2/3 complex is required for the formation of this actin structure. This phenotype was rescued by the expression of the ARPC4-V5 construct in the *arpc4* mutant cells (**Figure 4C**). The reliance of this structure on the Arp2/3 complex, led us to further question whether these dots could represent endocytic membrane remodeling.

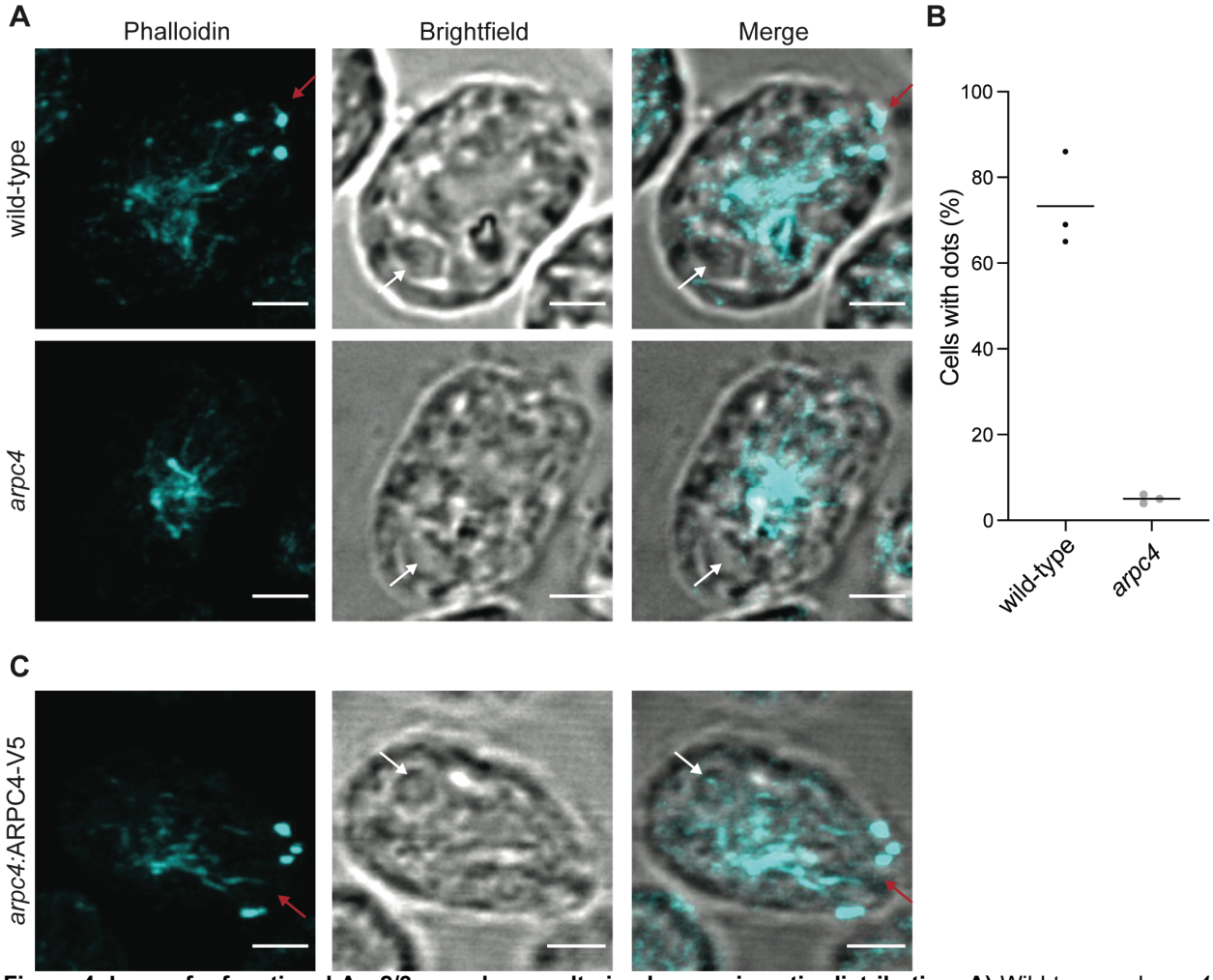

Figure 4. Loss of a functional Arp2/3 complex results in changes in actin distribution. A) Wild-type and *arpc4* mutant cells stained with phalloidin to visualize the actin network along with brightfield to show cell orientation. Images were taken as a z-stack using airsycan imaging and are shown as a maximum intensity projection. Red arrow is pointing to dots at the apex of the cell, and white arrow is pointing to the pyrenoid near the basal end of the cell. Scale bars represent 2μm. **B)** Percentage of cells with apical dots as shown in A. Percentages taken from 3 separate experiments where n=100. Line represents the mean. P<0.0001. **C)** Presence of apical dots in the *arpc4* mutant rescue expressing ARPC4-V5. Images were taken as a z-stack using airsycan imaging and are shown as a maximum intensity projection. Red arrow is pointing to dots at the apex of the cell, and white arrow is pointing to the pyrenoid near the basal end of the cell. Scale bars represent 2μm.

Endocytosis in *Chlamydomonas* is likely clathrin-dependent:

The Arp2/3 complex is conventionally thought to be involved in endocytosis in cell-walled yeast to overcome turgor pressure (Aghamohammadzadeh and Ayscough 2009; Basu, Munteanu, and Chang 2014; Carlsson and Bayly 2014). *Chlamydomonas* cells also have a cell wall and since the apical actin dots resemble these endocytic pits (Goode, Eskin, and Wendland 2015; Adams and Pringle 1984; Ayscough et al. 1997), we hypothesized that Arp2/3 complex and actin-dependent endocytosis might be occurring in *Chlamydomonas* even though this process has not yet been directly demonstrated in this organism. To determine what kind of endocytosis was likely occurring in these cells, we compared the endocytosis-related proteins found in mammals and plants to those in *Chlamydomonas* (**Figure 5A**). We found that *Chlamydomonas* lacks much of the important machinery for almost all typical endocytosis processes, including caveolin for caveolin-mediated endocytosis, flotillin for flotillin-dependent

342 endocytosis, and endophilin for endophilin-dependent endocytosis (**Figure 5A**). However, most
343 of the canonical clathrin-related endocytosis machinery could be found in *Chlamydomonas*, and
344 thus, clathrin-mediated endocytosis is conserved to a higher extent than other endocytic
345 mechanisms.
346 We aimed to further probe the likelihood of clathrin-mediated endocytosis occurring in
347 *Chlamydomonas.* However, a mutant for the proteins involved in clathrin-mediated endocytosis
348 does not currently exist and methods of targeted mutagenesis in *Chlamydomonas* are not yet
349 reliable. Therefore, we turned to our best alternative PitStop2, which inhibits the interaction of
350 adaptor proteins with clathrin, halting clathrin endocytosis, despite the reported off-target effects
351 on global endocytosis in mammalian cells (Willox, Sahraoui, and Royle 2014) (**Supplemental**
352 **Figure 4**). Additionally, we used the dynamin inhibitor Dynasore, which is also thought to block
353 endocytosis by inhibiting the GTPase activity of dynamin (Macia et al. 2006). For this
354 experiment, we used the fixable lipophilic dye FM 4-64FX (Cochilla, Angleson, and Betz 1999;
355 Gachet and Hyams 2005) (Thermo Scientific). This dye is impermeable to the plasma
356 membrane but is usually quickly endocytosed into cells showing bright foci where dye is
357 enriched in endocytosed compartments. Thus, we incubated the dye for only 1 minute to allow
358 enough time for internalization into endosomes but not enough for incorporation into various
359 cellular membrane structures. The ability of PitStop2-treated cells to internalize membrane was
360 measured by calculating the total cell fluorescence inside the cell after allowing dye to be
361 internalized (**Figure 5B**). We found that cells treated with 30μM PitStop2 or 100μM Dynasore
362 have significantly decreased membrane internalization (**Figure 5C**), which further supports the
363 idea that endocytosis of some kind is occurring in these cells and that it is likely clathrin-
364 mediated.
365 Next, we tested whether the endocytosis is Arp2/3 complex-dependent by using this
366 membrane internalization assay on *arpc4* mutant cells compared to wild-type cells. We found
367 that cells lacking a functional Arp2/3 complex have decreased total cell fluorescence (**Figure**
368 **5D-E**) suggesting the endocytosis in *Chlamydomonas* is Arp2/3 complex-dependent.
369 To better demonstrate the relationship between the Arp2/3 complex and endocytosis, we
370 used a clathrin light chain antibody to stain cells. In both PitStop2 treated cells and *arpc4* mutant
371 cells, but not in untreated wild-type cells, we see a mislocalization of clathrin staining around the
372 pyrenoid (**Supplemental Figure 8, Figure 5F-G**). Although the reason for this accumulation of
373 clathrin around the pyrenoid is not clear, the interesting takeaway from this data is that
374 disruption of either endocytosis with PitStop2 or of Arp2/3 function results in defects in
375 membrane internalization and clathrin localization. These data support a role for the Arp2/3
376 complex in endocytosis in *Chlamydomonas*.
377

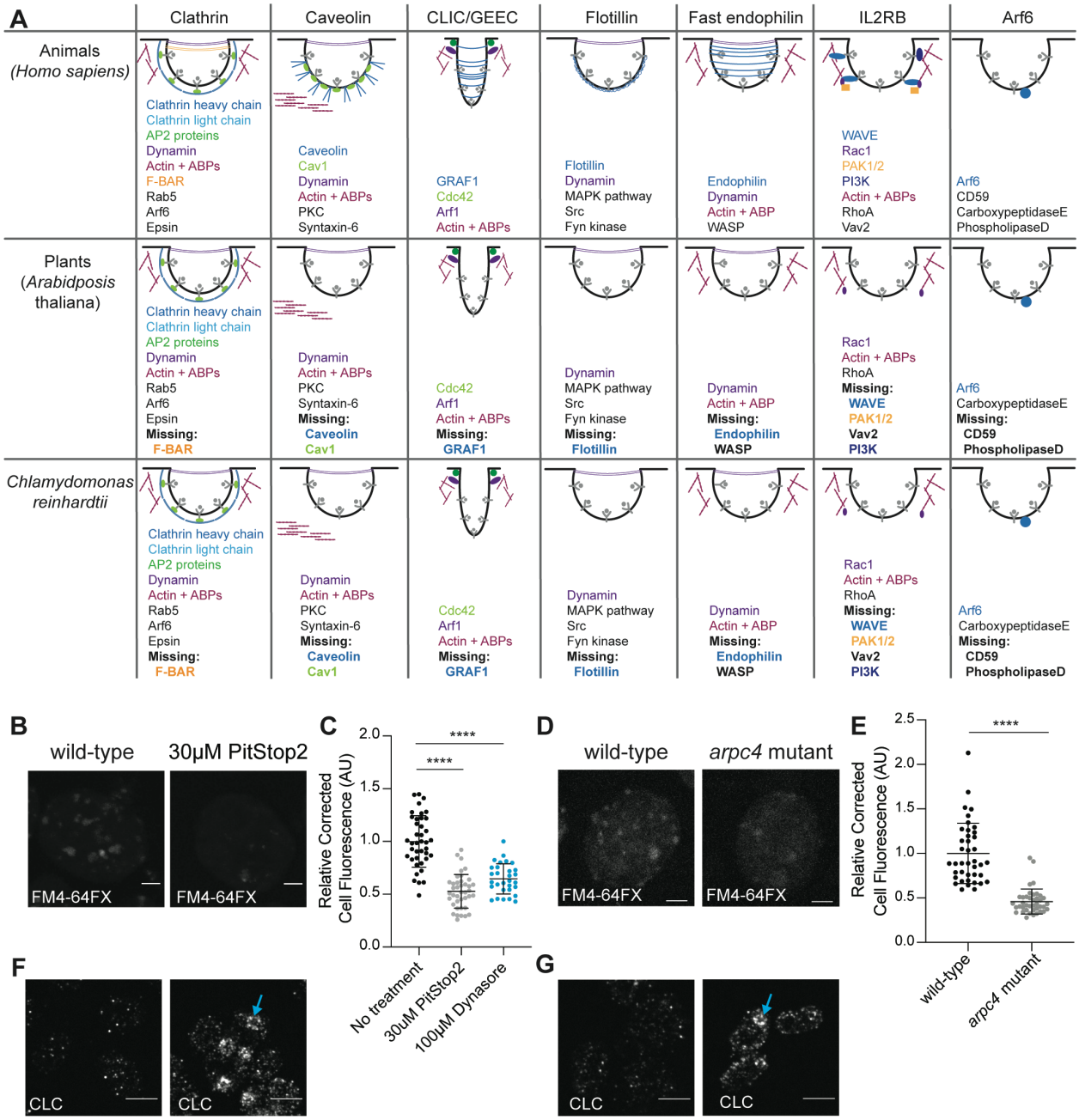

Figure 5. Arp2/3 complex-dependent endocytosis is conserved in *Chlamydomonas*. A) Gene presence was determined using BLAST. Word colors correspond to diagram colors. **B)** Cells treated with 30μM PitStop2 were incubated with FM4-64FX and imaged on a spinning disk confocal. Max intensity projections of z-stacks are shown. Scale bars are 2μm. **C)** The background corrected fluorescence for each sample, including cells treated with 100μM Dynasore. The mean is shown with error bars showing standard deviation. n=30 in 3 separate experiments. P<0.0001. **D)** Wild-type and *arpc4* mutant cells treated with FM4-64FX and imaged on a spinning disk confocal. Max intensity projections of z-stacks are shown. Scale bars are 2μm. **E)** The background corrected fluorescence for each sample. The mean is shown with error bars representing standard deviation. n=30 in 3 separate experiments. P<0.0001. **F)** Wild-type and PitStop2 treated cells, and arpc4 mutant cells were stained with clathrin light chain antibody and imaged using a spinning disk confocal. Cyan arrows point to accumulation around the pyrenoid. Scale bar represents 5μm. **G)** Wild-type and arpc4 mutant cells were stained with clathrin light chain antibody and imaged using a spinning disk confocal. Cyan arrows point to accumulation around the pyrenoid. Scale bar represents 5μm.

The Arp2/3 complex is required for the internalization and relocalization of a membrane protein from the periphery of the cell to cilia:

Upon finding that there is likely Arp2/3 complex-dependent clathrin-mediated endocytosis in *Chlamydomonas*, we next asked if this endocytosis could be responsible for the relocalization and internalization of a known ciliary protein. SAG1 is a membrane protein that is important for mating in *Chlamydomonas* cells (Belzile et al. 2013; Ranjan, Awasthi, and Snell 2019). When cells are induced for mating with dibutyryl-cAMP (db-cAMP), SAG1 must relocalize from the cell periphery to cilia, where it facilitates ciliary adhesion between mating cells. This relocalizaiton of SAG1 is thought to occur through internalization of the protein followed by internal trafficking on microtubules to the base of cilia (Belzile et al. 2013; Ranjan, Awasthi, and Snell 2019).

We examined whether actin and the Arp2/3 complex were required for the transport of HA-tagged SAG1 to the apex of the cell and cilia for agglutination during mating (**Figure 6A**). Using immunofluorescence, we observed cells treated with either 10μM LatB to depolymerize IDA5 or 250μM CK-666 to perturb the Arp2/3 complex (**Figure 6, Supplemental Figure 4**). Before induction, SAG1-HA localized to the periphery of the cell (**Figure 6B, top**). 30 minutes after induction with db-cAMP, SAG1-HA relocalized to the apex of the cell and to cilia in untreated cells (**Figure 6B, left**). In both LatB and CK-666 treated cells, this apical enrichment was greatly decreased (**Figure 6B, middle and right**). To quantify this, line scans were drawn through the cell from the apex to the basal region (**Figure 6C-D**). The percentage of cells with apical enrichment was calculated, and it was found that untreated cells had a higher percent of apical enrichment when compared with LatB or CK-666 treated cells (**Figure 6E**). Thus, cells with perturbed Arp2/3 complex-mediated filamentous actin show decreased efficiency of SAG1-HA relocalization.

We next asked if this decrease in relocalization in cells with actin and Arp2/3 complex inhibition could be due to a decrease in the internalization of SAG1-HA through a process that seems to require endocytosis. To investigate this, we used a method first described by Belzile et al. 2013, where cells were induced and treated with a low percentage (0.01%) of trypsin, which will hydrolyze exterior proteins but cannot enter the cell. In untreated cells, we see an increase in SAG1-HA protein levels following induction because SAG1-HA is internalized and becomes protected from trypsin (**Figure 6F**). In cells treated with either 10μM LatB or 250μM CK-666 we see a decrease in this trypsin protection as shown in the western blot (**Figure 6F**). This was further quantified by subtracting the amount of protein before induction from the amount of protein present after induction, which gives a value representing the amount of SAG1-HA protected from trypsin due to internalization in these cells (**Figure 6G**). The decrease in SAG1-HA following induction in cells with decreased filamentous actin and Arp2/3 complex function indicates a role for Arp2/3 complex-mediated actin networks in internalization of this specific ciliary membrane protein.

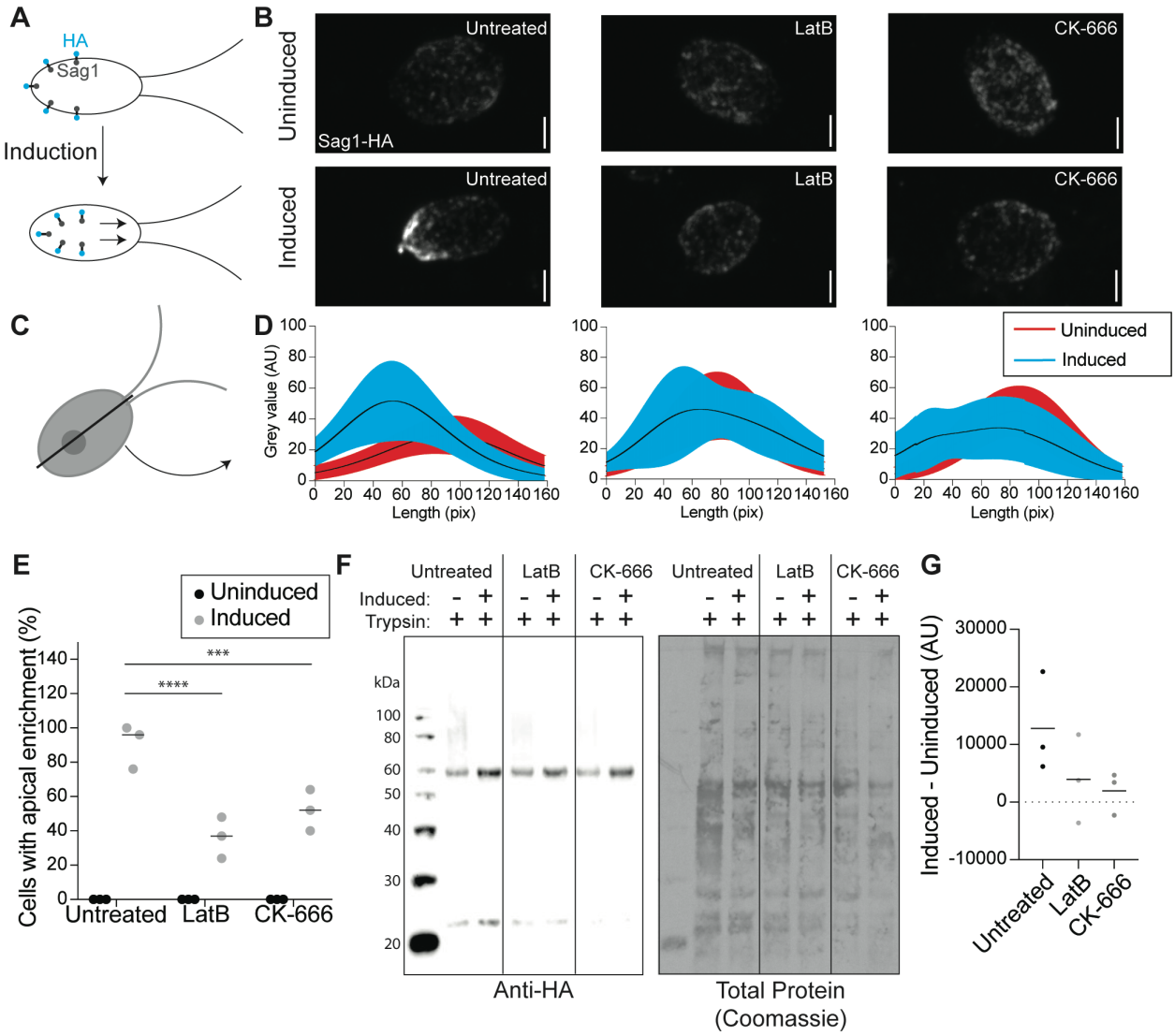

Figure 6. The Arp2/3 complex is required for the relocalization and internalization of the ciliary protein SAG1 for mating. A) When mating is induced SAG1-HA is internalized and relocalized to the apex of the cells and cilia for agglutination. **B)** Maximum intensity projections of z-stacks taken using spinning disk confocal microscopy of SAG1-HA. Left is untreated, middle is treated with 10μM LatB, and right is treated with 250μM CK-666. Top row of images are uninduced and bottom row of images are induced with db-cAMP. Scale bar represents 2μm. **C)** Diagram representing line scans taken through the cells in z-stack sum images. **D)** Line scans were taken from the apex of the cell to the basal region of the cell in untreated cells (left), LatB treated cells (middle), and CK-666 (right). Lines scans were normalized and fit with a gaussian curve. The curves were averaged. Black lines represent mean and then shaded regions represent standard deviation. Grey represents uninduced samples, green represent induced samples. 0 on the y-axis represents the apical region of the cell. n=30 from a single representative experiment. **E)** Percentage of cells with apical enrichment based on E for uninduced (black) and induced (grey) cells for each treatment group. The mean is shown with error bars representing standard deviation. n=30 for 3 separate experiments for each treatment. **F)** Western blot showing amount of SAG1-HA in uninduced and induced cells in each treatment group all treated with 0.01% trypsin. **G)** Intensity of the bands in H were normalized to the total protein as determined by amido black staining and quantified in ImageJ was used to subtract uninduced from induced to give a representation of the amount of SAG1-HA internalized with induction. Line represents mean of 3 separate experiments.

Actin dots increase in an Arp2/3 complex and clathrin-dependent manner following deciliation:

453 Having established that the Arp2/3 complex is required for ciliary assembly, membrane
454 dye internalization, and the endocytosis of a known ciliary protein, we wondered if these
455 functions could be connected given that *arpc4* mutant cells have defects in maintaining cilia
456 from non-Golgi sources (**Figure 3**). Therefore, we returned to the Arp2/3 complex-dependent
457 actin dots seen in wild-type cells that are reminiscent of endocytic pits in yeast. Because ciliary
458 membrane and proteins can come from the plasma membrane (Dentler, 2013), we suspected
459 there would be an increase in these actin dots immediately following deciliation. We used
460 phalloidin to visualize the actin cytoskeleton of wild-type cells before and immediately following
461 deciliation, as well as 10 minutes later (**Figure 7A**). We saw an increase in both the percentage
462 of cells with dots and the number of dots per cell immediately following deciliation that then
463 returned to normal by 10 minutes (**Figure 7A and D**). This is consistent with the results shown
464 in **Figure 1E-F** and confirms that the defect seen in ciliary assembly is due to an event
465 occurring very early in ciliary assembly, even within the first few minutes after deciliation.
466 We wondered if this increase in dots would result in dots in the *arpc4* mutant cells which
467 have almost not dots normally. We found that in the *arpc4* mutants dots were never observed,
468 before or after deciliation (**Figure 7B and D**), suggesting these dots are dependent on the
469 Arp2/3 complex. Next, we wanted to see if the dots really were due to clathrin-mediated
470 endocytosis, so we treated cells with PitStop2 and looked for this same increase in dots. This
471 treatment almost fully blocked the appearance of dots following deciliation and completely
472 eliminated the presence of cells with 3 or more dots (**Figure 7C-D**), suggesting a clathrin-
473 dependent mechanism, as well as an Arp2/3-dependent mechanism, is related to these dots.
474

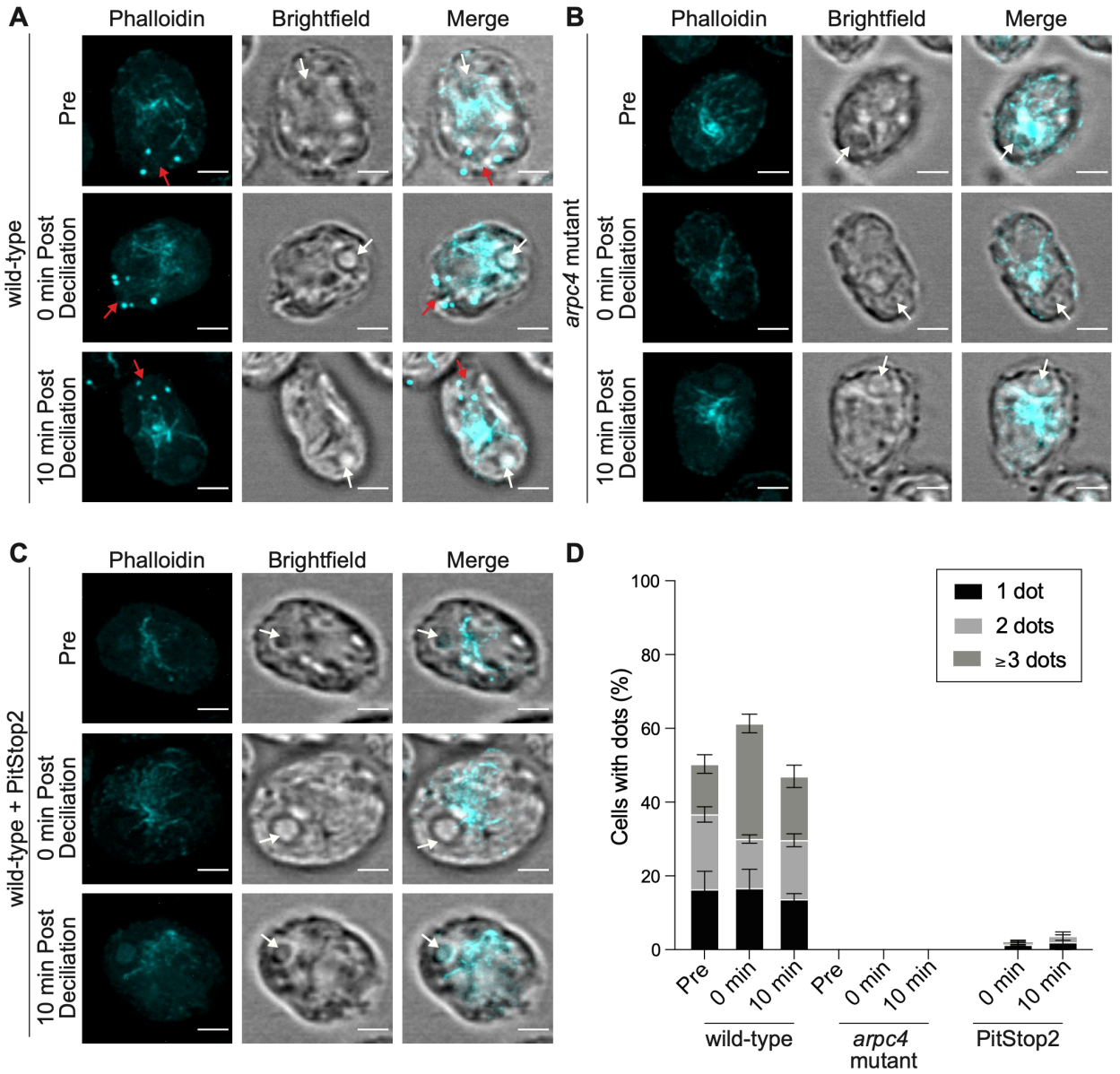

Figure 7. Actin dots are clathrin and Arp2/3 complex-dependent. A-C) Wild-type cells **(A)**, *arpc4* mutant cells **(B)**, and wild-type cells treated with 30 µM PitStop2 **(C)** stained with phalloidin to visualize the actin network before deciliation, immediately following deciliation, and 10 minutes following deciliation. Brightfield images are to visualize cell orientation. Images were taken as a z-stack using airyscan imaging and are shown as a maximum intensity projection. Scale bar represents 2µm. Red arrows point to dots at the apex of the cell, and white arrows point to the pyrenoid at the opposite end of the cell. **D)** The percentage of cells with 1 dot, 2 dot, or 3 dots in each condition. Quantification based on sum slices of z-stacks taken using a spinning disk confocal. n=100 in 3 separate experiments. For wild-type, the total number of cells with dots is significantly different for the 0 min time point (**) and the number of dotted cells with 3 or more dots is significantly different for the 0 time point (****).

Ciliary membrane proteins follow different paths from the plasma membrane to the cilia:

Finally, to specifically determine if ciliary membrane and therefore membrane proteins were coming from a pool in the plasma membrane we did an experiment first described in W. Dentler 2013. Surface proteins were biotinylated, then cells were deciliated. After the cilia regrew, they were isolated and probed for biotinylated protein (**Figure 8A**). Any biotinylated

protein present in the newly grown and isolated cilia must have come from a pool in the plasma membrane. While some proteins returned in both wild-type and *arpc4* mutant cells, some appeared to a lesser degree in *arpc4* mutant cells compared to wild-type cells (**Figure 8B-E, black arrow and black bars**) and some returned to a higher degree in *arpc4* mutant cells (**Figure 8B-E, grey arrow and grey bars**). Other biotinylated proteins found in wild-type cilia were not found in the *arpc4* mutant cilia before or after deciliation, so there is a mechanism for delivery of proteins to the cilia from the plasma membrane that Arp2/3 is absolutely essential for (**Figure 8B-C**). This suggests there are multiple paths to the ciliary membrane, some of which are Arp2/3 complex-independent and some that are Arp2/3 complex-dependent. This may represent lateral diffusion and endocytosis respectively.

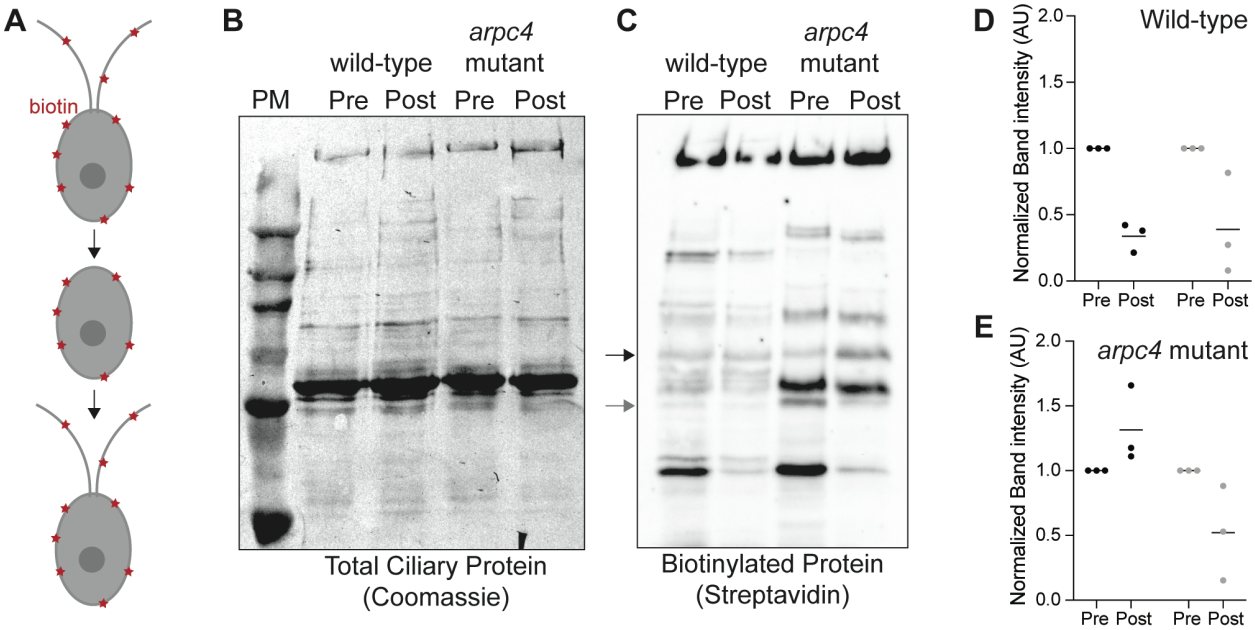

Figure 8. Ciliary membrane proteins have multiple paths from the plasma membrane. A) Cells were biotinylated, deciliated, and then allowed to regrow before cilia were isolated and probed for biotinylated protein**. B)** Total protein in wild-type and *arpc4* mutant ciliary isolate investigated by western blot and Coomassie. **C)** Wild-type and *arpc4* mutant cells ciliary isolate was investigated by western blot and probed using streptavidin. Black arrow shows ciliary protein present to a higher degree in wild-type cells than the *arpc4* mutant cells. Grey arrows show ciliary protein that is present to a higher degree in *arpc4* mutant cells than in wild-type cells. **D)** Bands represented by black and grey arrows are quantified for the wild-type cells. Data acquired from 3 separate experiments. **E)** Bands represented by black and grey arrows are quantified for the *arpc4* mutant cells. Data represented as the mean from 3 separate experiments. Error bars represent standard deviation.

DISCUSSION

In this study, we investigate the Arp2/3 complex of *Chlamydomonas reinhardtii* that functions to maintain and assemble cilia. This complex potentially lacks the ARPC5 subunit, although it is possible that a highly divergent ARPC5 exists. In yeast, deletion of any of the genes encoding Arp2/3 complex members causes severe defects and even lethality, but these defects differ in severity depending on the complex members deleted, suggesting that complex members have varying degrees of importance in Arp2/3 complex function (Winter, Choe, and Li 1999). The role of ARPC5 in actin nucleation is being investigated, but some groups have found it unnecessary for overall function of the complex (Gournier et al. 2001; von Loeffelholz et al. 2020). Furthermore, our data show that knocking out function of the ARPC5-less

528 *Chlamydomonas* Arp2/3 complex genetically or chemically results in phenotypes in ciliary
529 assembly and maintenance, suggesting that the wild-type complex is active. Because the
530 Arp2/3 complex has known functions in membrane dynamics, this led us to pursue models of
531 Arp2/3 complex-dependent membrane trafficking to cilia.
532 Previously, three models for the trafficking of membrane proteins to cilia have been
533 proposed regarding where ciliary vesicles fuse relative to a diffusion barrier composed of
534 septins (Hu Qicong et al. 2010), which delineates ciliary membrane and cell body plasma
535 membrane (Nachury, Seeley, and Jin 2010). The first is that Golgi vesicles containing ciliary
536 proteins fuse with the ciliary membrane inside the cilium itself. Proteins, both membrane and
537 soluble, have been found to be transferred from the Golgi to the cilia on or in cytoplasmic
538 vesicles (Wood and Rosenbaum 2014). Second, Golgi vesicles containing ciliary proteins fuse
539 outside but near the cilium still within the diffusion barrier (Papermaster, Schneider, and
540 Besharse 1985; Nachury et al. 2007; Zuo, Guo, and Lipschutz 2009). In *Chlamydomonas*, this
541 was first described for mastigoneme proteins, which were found to be transferred from the Golgi
542 and then exocytosed for use on the exterior of the cell (Bouck 1971). In the third model, Golgi
543 vesicles containing proteins fuse with the plasma membrane outside the diffusion barrier where
544 they somehow move in the plane of the plasma membrane across this barrier, perhaps through
545 lateral diffusion that requires remodeling or passing through the diffusion barrier. Evidence for
546 this path was shown using Hedgehog signaling protein Smoothened, which was found to
547 relocalize in a dynamin-independent manner from the plasma membrane to the cilia
548 immediately after stimulation in pulse labeling studies (Milenkovic, Scott, and Rohatgi 2009).
549 Our data support a fourth model, likely occurring in concert with other models, in which
550 membrane proteins are recruited to the cilium from a reservoir in the cell body plasma
551 membrane. We find that immediately following deciliation the Arp2/3 complex is required for
552 ciliary assembly, clathrin-mediated endocytosis, and redistribution of ciliary proteins from the
553 plasma membrane (**Figure 9A**). We hypothesize that ciliary membrane proteins and membrane
554 targeted to the plasma membrane of the cell outside the diffusion barrier can be endocytosed
555 and trafficked to cilia, either within or outside of the diffusion barrier in an actin and Arp2/3
556 complex-dependent manner.
557 Although our data does not eliminate the possibility of Arp2/3 complex function in supply
558 of ciliary membrane and protein stored in other endosomal compartments, ciliary localization of
559 proteins initially labeled on the cell surface with biotin (**Figure 8**) suggests that some ciliary
560 membrane proteins incorporated during assembly are coming directly from the plasma
561 membrane itself. An endocytic mechanism of trafficking in intracellular ciliogenesis has been
562 investigated previously in mammalian RPE1 cells. The ciliary pocket found at the base of
563 primary and motile cilia formed intracellularly has been found to be an endocytically active
564 region (Molla-Herman et al. 2010) but clathrin-mediated endocytosis was not required for
565 ciliogenesis in those cells. The Bardet Biedl Syndrome complex (BBsome), which is involved in
566 regulation of ciliary membrane protein composition, has been shown to interact with clathrin
567 directly at the ciliary pocket to facilitate membrane sorting in trypanosomes (Langousis et al.
568 2016). Further, some BBsome complex members resemble coat proteins such as clathrin (Jin et
569 al. 2010) suggesting a direct role for the this cilium regulatory complex in membrane budding
570 functions. It has also been found that disruption of recycling endosomes reduces the localization
571 of polycystin-2 to cilia, suggesting a role for recyclying endosomes in the localization of proteins
572 to the cilia (Monis, Faundez, and Pazour 2017). Even in *Chlamydomonas*, clathrin heavy chain
573 has been found to localize at the base of cilia (Kaplan et al. 2012). While the mechanism was
574 unknown, it has been shown that plasma membrane surface-exposed proteins are relocalized to
575 cilia during ciliary regeneration (W. Dentler 2013), a result we were able to recapitulate and
576 demonstrate depends, in part, upon the Arp2/3 complex.
577 Altogether, this leads us to hypothesize that the role of the Arp2/3 complex in ciliary
578 assembly is through endocytic recruitment from a ciliary protein reservoir in the plasma

membrane before newly synthesized protein and Golgi-derived membrane are capable of supplying additional materials (**Figure 9B**). While this model provides a possible route that some ciliary proteins and membranes take to the cilia, we believe this is one of several paths that can be taken to the cilia. Trafficking to cilia is likely cargo- and time-dependent, and which path proteins take may tell us the order and speed in which they populate the cilium for subsequent function.

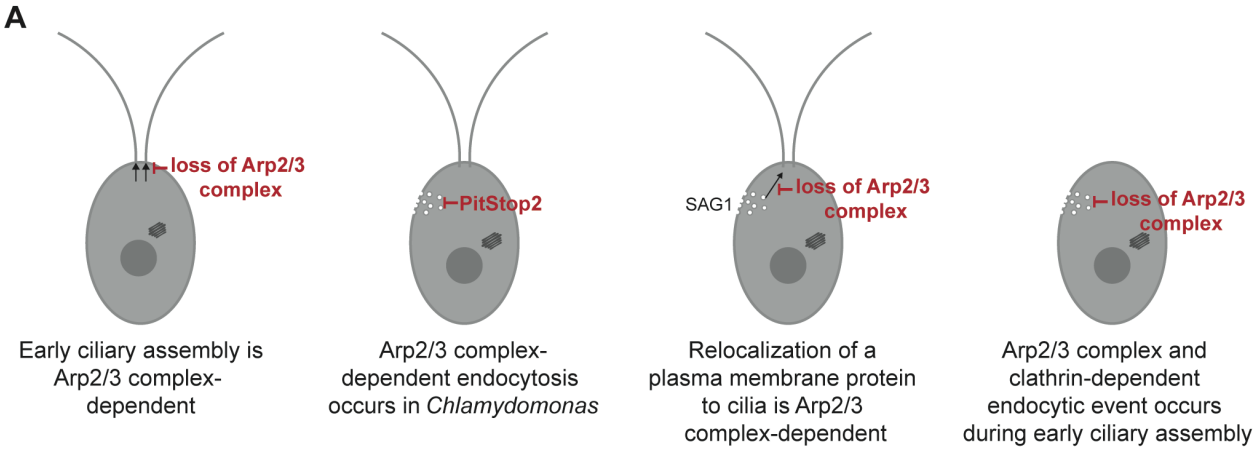

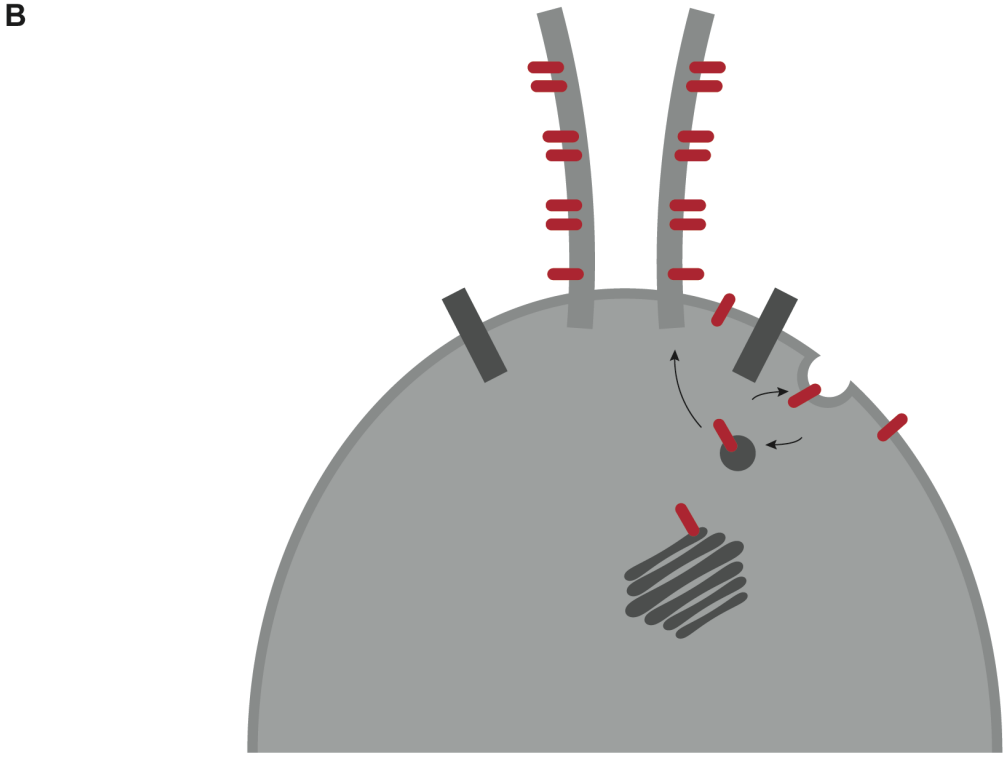

Figure 9. The Arp2/3 complex is required for membrane and protein delivery via a Golgi-independent, endocytosis-like process. A) Arp2/3-mediated actin networks are required for ciliary assembly in *Chlamydomonas* particularly during the initial stages. These actin networks are also required for clathrin-mediated endocytosis, and for the endocytosis-like relocalization of a ciliary protein from the plasma membrane to the cilia. Finally, a large endocytic event occurs immediately following deciliation that is Arp2/3 complex-mediated and dependent on clathrin-mediated endocytosis. **B)** Proposed model of membrane protein and membrane transport from the plasma membrane to the cilia through endocytosis.

METHODS

Strains:

The wild-type *Chlamydomonas* strain (CC-5325) and the *arpc4* mutant (LMJ.RY0402.232713) from the *Chlamydomonas* resource center. The *arpc4:*ARPC4-V5 strain was made by cloning the gene into pChlamy4 (*Chlamydomonas* resource center). Colonies were screened for the absence (in the case of the mutant) or presence (in the case of the rescue) by PCR using the primers AAAAGAATTCATGGCGCTCTCACTCAGGCCATA and AAAATCTAGACAGAAGGCAAGGGAGCGCAGGAA. The *nap1* mutant was a gift from Fred Cross, Masayuki Onishi, and John Pringle. The SAG1-HA strain was a gift from William Snell. Cells were grown and maintained on 1.5% Tris-Acetate Phosphate Agar (TAP) plates (*Chlamydomonas* resource center) under constant blue (450-475 nm) and red light (625-660 nm). For experiments, cells were grown in liquid TAP media (*Chlamydomonas* resource center) overnight under constant red and blue light with agitation from a rotator. To induce gametes for mating for the SAG1-HA experiments, cells were grown in liquid M-N media (*Chlamydomonas* resource center) overnight with constant red and blue light and agitation.

Ciliary studies:

For steady state experiments, cells were treated with specified drugs [either 100μM CK-666, 250μM CK-666 (Sigma, Burlington, MA), 250μM CK-689 (Sigma, Burlington, MA), 10μM LatB (Sigma, Burlington, MA), 10μM CHX (Sigma, Burlington, MA), or 36μM BFA (Sigma, Burlington, MA)] and incubated with agitation for the allotted times. Following any incubation (as well as a pre sample), cells were diluted in an equal volume of 2% glutaraldehyde and incubated at 4º Celsius until they sediment (within 24hrs). Following sedimentation, cells were imaged using a Zeiss DIC scope with a 40X objective. Cilia were then measured using the segmented line function in ImageJ. One cilia per cell was measured and 30 cilia total were measured.

For regeneration experiments, a pre sample was taken by adding cells to an equal volume of 2% glutaraldehyde. Then cells were deciliated with 115μL of 0.5N acetic acid for 45 seconds. After this short incubation, the pH was returned to normal by adding 120μL of 0.5N KOH. A 0-minute sample was again taken by adding cells to an equal volume of 2% glutaraldehyde. Then cells were incubated with agitation and allowed to regrow cilia for the allotted time period with samples taken at the indicated time points by adding cells to an equal volume of 2% glutaraldehyde. Cells in glutaraldehyde were allowed to incubate at 4º Celsius until sedimentation (within 24hrs). Then, cells were imaged using the same Zeiss DIC scope with a 40X objective. Cilia were then measured using the segmented line function in ImageJ. One cilia per cell was measured and 30 cilia total were measured.

Click-iT OPP Protein Synthesis Assay:

Cells were grown overnight in TAP. The following day cells were deciliated as described above and allowed to regrow either with or without cycloheximide (10μM) to block protein synthesis. 1 hour following deciliation, cells were mounted onto poly-lysine coverslips. Cells on coverslips were incubated with Click-iT OPP reagent containing the O-propargyl-puromycin (OPP) which is incorporated into nascent polypeptides for 30 minutes. OPP was removed and cells were

644 washed once in PBS. Cells were then fixed with 4% PFA in 1X HEPES for 15 minutes, then
645 permeabilized with 0.5% Triton-X 100 in PBS for 15 minutes. Cells were washed twice with
646 PBS. Detection was performed by incubating coverslips with 1X Click-iT OPP Reaction Cocktail
647 that includes 1X Click-iT OPP Reaction Buffer, 1X Copper Protectant, 1X Alexafluor picolyl
648 azide, and 1X Click-iT Reaction Buffer Additive for 30 minutes protected from light. This was
649 removed and Reaction Rinse Buffer was added for 5 minutes. This was removed and coverslips
650 were washed twice with PBS, allowed to dry fully, and mounted with Fluormount-G.
651
652 Cells were then imaged on a Nikon Spinning Disk Confocal. Z-stacks were obtained then
653 combined into sum slices for quantification of maximum intensity projections for viewing. In the
654 summed images, the integrated density and area of individual cells was obtained, as well as the
655 background fluorescence. These were then used to calculate CTCF, which was then normalized
656 to the "Pre" sample for each cell.
657
658 *Phalloidin staining and quantification:*
659 Procedure adapted from (Craig et al. 2019). Cells were mounted onto poly-lysine coverslips and
660 fixed with fresh 4% paraformaldehyde in 1X HEPES. Coverslips with cells were then
661 permeabilized with acetone and allowed to dry. Cells were rehydrated with PBS, stained with
662 atto-phalloidin-488 (Sigma, Burlington, MA), and finally washed with PBS and allowed to dry
663 before mounting with Fluoromount-G (Craig et al. 2019). Cells were imaged using the Nikon
664 Spinning Disk Confocal. Z-stacks were obtained, and in ImageJ, maximum intensity projections
665 were created for viewing.
666
667 *Electron microscopy:*
668 Cells (1mL of each strain) were deciliated via pH shock by adding 115μL of 0.5N acetic acid for
669 45 seconds followed by 120μL of 0.5N KOH to bring cells back to neutral pH. Cells were
670 allowed to regrow cilia for 30 minutes. A pre sample and a 30-minute post-deciliation sample
671 were fixed in an equal volume of 2% glutaraldehyde for 20 minutes at room temperature.
672 Samples were then pelleted using gentle centrifugation for 10 minutes. The supernatant was
673 removed, and cells were resuspended in 1% glutaraldehyde, 20mM sodium cacodylate. Cells
674 were incubated for 1 hour at room temperature and then overnight at 4º Celsius. This protocol
675 was first reported in (W. L. Dentler and Adams 1992).
676
677 *SAG1-HA Immunofluorescence:*
678 Procedure adapted from (Belzile et al. 2013). SAG1-HA cells were grown overnight in M-N
679 media to induce gametes. These cells were then treated with either 10μM LatB for 1 hour or
680 250μM CK-666 for 2 hours. Following treatment, mating was induced by adding db-cAMP
681 (ChemCruz, Santa Cruz, CA) to a final concentration of 13.5mM and incubating for 30 minutes.
682 Cells were adhered to coverslips and fixed with methanol. Cells were then dried and rehydrated
683 with PBS and incubated with 100% block (5% BSA, 1% fish gelatin) for 30 minutes. The 100%
684 block was replaced with new 100% block containing 10% normal goat serum for another 30-
685 minute incubation. The primary antibody (rat anti-HA, Sigma, Burlington, MA) was diluted
686 1:1000 in 20% block in PBS. Coverslips were incubated at 4º Celsius in a humidified chamber
687 overnight. The primary antibody was removed and washed away with 3 10-minute PBS washes.
688 The secondary (anti-rat IgG-Alexafluor 488, Invitrogen, Carlsbad, CA) was added and coverslips
689 were incubated at room temperature for 1 hour. This was followed by 3 more 10-minute PBS
690 washes and finally mounting with Fluoromount-G. Cells were imaged using a Nikon widefield
691 microscope. Z-stacks were obtained, and maximum intensity projections were created for
692 visualization and sum slices were created for quantification using ImageJ.
693

694 Images were quantified by using line scans from the apex of the cells to the basal region of the
695 cells farthest away from the apex. Line scans were then normalized, and background subtracted
696 before being combined into single graphs. Using the line scans, the intensity of signal at the
697 basal region of the cells was subtracted from the signal at the apical region. Finally, cells with a
698 difference over 30 were considered to be apically enriched and this was quantified as
699 percentage of cells with apical staining.
700
701 *SAG1-HA western blot:*
702 Procedure adapted from (Belzile et al. 2013). SAG1-HA cells were grown overnight in M-N
703 media to induce gametes. These cells were then treated with either 10μM LatB for 1 hour or
704 250μM CK-666 for 2 hours. Following treatment, mating induction was done by adding db-cAMP
705 to a final concentration of 13.5mM and incubating for 10 minutes. Cells were then treated with
706 0.01% trypsin for 5 minutes, pelleted (at 500xg for 2 minutes), resuspended in lysis buffer (5%
707 glycerol, 1% NP-40, 1mM DTT, 1X protease inhibitors), and then lysed with bead beating. Cell
708 debris was spun down at 14000xg for 15 minutes. An equal amount of protein was loaded to a
709 10% SDS-PAGE gel. The resulting gel was transferred to membrane which was then blocked
710 with 5% milk in PBST. The primary antibody (rabbit anti-HA, Cell Signaling, Danvers, MA)
711 diluted to 1:1000 in 1% BSA, 1% milk was added and incubated overnight at 4º Celsius. Primary
712 antibody washed off with 3 10-minute PBST washes. Secondary antibody (anti rabbit IgG,
713 Invitrogen, Carlsbad, CA) was diluted to 1:5000 in 1% milk. 1% BSA was added, and the blot
714 was incubated for 1 hour. Membrane was probed with West Pico Chemiluminescent Pico
715 Substrate (Invitrogen, Carlsbad, CA). The same membrane was stripped of antibody and total
716 protein was determined with amido black staining. Band intensity was measured in ImageJ and
717 normalized to total protein
718
719 *Membrane stain:*
720 FM 4-64FX membrane stain (Thermo, Waltham, MA) was diluted to a stock concentration of
721 200μg/mL. Cells were adhered to poly-lysine coverslips. After a 5-minute incubation, cells were
722 tilted off and 5μg/mL of ice-cold stain in Hank's Buffered Salt Solution (HBSS) without
723 magnesium or calcium was added for 1 minute. The stain was tilted off and cells were fixed with
724 ice cold 4% paraformaldehyde in HBSS without magnesium or calcium for 15 minutes.
725 Coverslips were then rinsed 3 times for 10 minutes each in ice cold HBSS without magnesium
726 or calcium. Finally, cells were mounted with Fluoromount-G and imaged using the Nikon
727 Spinning Disk Confocal. Z-stacks were taken and combined into sum projections using ImageJ.
728 The background corrected total cell fluorescence was then calculated by taking the integrated
729 density and subtracting the sum of the area and the mean background intensity.
730
731 *Clathrin light chain immunofluorescence:*
732 Cells were grown overnight in TAP media. Cells were deciliated using low pH shock. Cells are
733 then adhered to coverslips and fixed with 4% PFA in 1X HEPES. Cells were then dried and
734 rehydrated with PBS and incubated with 100% block (5% BSA, 1% fish gelatin) for 1 hour. The
735 primary antibody (goat anti-clathrin light chain, Abcam, Cambridge, UK or rabbit anti-acetylated
736 tubulin, Cell Signaling, Danvers, MA) was diluted 1:1000 in 20% block in PBS. Coverslips were
737 incubated at 4º Celsius in a humidified chamber overnight. The primary antibody was removed
738 and washed away with 3 10-minute PBS washes. The secondary (donkey anti-goat IgG-
739 Alexafluor 488, Invitrogen, Carlsbad, CA or goat anti-rabbit IgG-Alexafluor 568, Invitrogen,
740 Carlsbad, CA) was added and coverslips were incubated at room temperature for 1 hour. For
741 cells stained with DAPI, DAPI (Biotium, Fremont, CA) was added for the last 10 minutes of
742 secondary antibody incubation. This was followed by 3 more 10-minute PBS washes and finally
743 mounting with Fluoromount-G. Cells were imaged using a Nikon widefield microscope. Z-stacks

744 were obtained, and maximum intensity projections were created for visualization and sum slices
745 were created for quantification using ImageJ.
746
747 *Biotin ciliary isolation:*
748 Procedure adapted from (W. Dentler 2013). 100mL of cells were grown in TAP for each
749 condition until they reached an OD_{730} of 1.6 or above. Cells were then spun down and
750 resuspended in M1 media and allowed to grow overnight. The next day cells were spun down at
751 1800rpm for 3 minutes and resuspended in HM Media (10mM HEPES, 5mM MgSO4, pH 7.2).
752 Solid biotin (Thermo, Waltham, MA) was added to 20µg/mL for each strain and incubated for 5
753 minutes with agitation. Cells were diluted with 10 volumes of fresh M1 media before being spun
754 down at 1800rpm for 3 minutes. After all cells were pelleted, they were washed with fresh M1
755 media three times. A pre sample was set aside (100mL) and the remainder of the cells were
756 resuspended in 4.5 pH M1 media for 45 seconds before being spun down again at 1800rpm for
757 3 minutes. Cells were then resuspended in pH 7.0 media and allowed to regrow their cilia for 4
758 hours. A sample was taken pre-biotinylation to use as a control for non-specific streptavidin
759 binding.
760
761 Meanwhile, the cilia were isolated from the pre sample. The samples were centrifuged for 3
762 minutes at 1800rpm. Supernatant was drained and each pellet was resuspended in 2 mL of
763 10mM HEPES (pH 7.4). This was repeated 2 times. Then each pellet was resuspended in 1 mL
764 of fresh ice-cold 4% HMDS (10mM HEPES pH 7.4, 5mM MgSO4, 1mM DTT, 4% w/v sucrose).
765 Cells were deciliated by incubating with 25mM dibucaine for 2 minutes. Then ice cold HMDS
766 with 0.5mM EGTA was added (1mL per 1.5mL of cells). This was then centrifuged for 3 minutes
767 at 1800rpm. Supernatant was collected for each sample. Then HMDS with 25% sucrose was
768 layered beneath the supernatant (2 mL of 25% HMDS for 1mL of supernatant) to create an
769 interface. This was centrifuged at 4º Celsius for 10 min at 2400rpm with no brake to avoid
770 disrupting interface where cilia should now be located. Cilia were removed, pelleted at 21130xg
771 for 30 minutes, then resuspended in lysis buffer (5% glycerol, 1% NP-40, 1mM DTT, 1X
772 protease inhibitors). This was repeated with the post samples 4 hours following deciliation. An
773 equal amount of protein was loaded to a 10% SDS-PAGE gel. The resulting gel was transferred
774 to PVDF membrane. The membrane was washed 2x with PBSAT (PBST + 0.1% BSA), then
775 incubated with HRP-conjugated streptavidin (Thermo, Waltham, MA) for 1 hour. The membrane
776 was then washed 3 times with PBSAT (10 minutes each) and 3 times with PBST (15 minutes
777 each). Membrane was probed with West Pico Chemiluminescent Pico Substrate (Invitrogen,
778 Carlsbad, CA). The same membrane was stripped of antibody and incubated with Coomassie
779 Brilliant Blue to observe total protein.
780
781 *Homology modeling and sequence studies:*
782 Arp2/3 homology model was created using the Modeller plugin in UCSF Chimera. The template
783 used was 1U2Z (Nolen, Littlefield, and Pollard 2004; Sali and Blundell 1993; Pettersen et al.
784 2004). Percent identity and similarity is calculated in relation to the human Arp2/3 complex
785 members using a MUSCLE alignment in Geneious. The homology model was visualized and
786 conservation was mapped on the protein surface using Chimera (Pettersen et al. 2004).
787
788 *Statistical analysis:*
789 Statistical analyses were done if GraphPad Prism Version 9. Superplots were created using the
790 method in (Lord et al. 2020). For any experiments comparing 2 groups (**Figure 3D, 5C, and 5E**)
791 an unpaired student's t-test was used to determine P value. For experiments comparing multiple
792 samples at a single time point (**Figure 1A, 1B, and 2B**), an ANOVA was used. Finally, for any
793 graphs covering several time points (**Figure 1C, 1D, 2C, 3B, and 6E),** multiple comparisons

were performed (Tukey's and Sidak's). For any percentages shown (**Figure 7D**), Chi-squared analysis was performed. For all experiments **** P<0.0001, *** P<0.001, ** P<0.01, * P<0.1.

ACKNOWLEDGEMENTS:

Our most sincere gratitude to William Dentler for providing his expertise especially in looking at the electron microscopy images and for his helpful advice, William Snell for generously providing the SAG1-HA strain, Masayuki Onishi for generously providing the *nap1* mutant strain, Henry Higgs for his feedback on version 1 of the manuscript, Ann Lavanway for assistance with microscopy, and the Avasthi lab for all their help throughout the project. We would also like to thank David Sept and Courtney M Schroeder for the help with the original version of this paper and for providing helpful comments throughout the process.

We also thank our funding sources including the Madison and Lila Self Graduate Fellowship at the University of Kansas Medical Center and the MIRA (R35GM128702). Finally, we thank the BioMT core at Dartmouth College (NIH/NIGMS COBRE award P20-GM113132), the Genomics and Molecular Biology Shared Resources Core (NCI Cancer Center Support Grant 5P30CA023108-37), and the KIDDRC NIH U54 HD 090216 at the University of Kansas Medical Center, Kansas City, KS 66160.

REFERENCES:

Adams, A E, and J R Pringle. 1984. "Relationship of Actin and Tubulin Distribution to Bud Growth in Wild-Type and Morphogenetic-Mutant Saccharomyces Cerevisiae." *Journal of Cell Biology* 98 (3): 934–45. https://doi.org/10.1083/jcb.98.3.934.

Aghamohammadzadeh, Soheil, and Kathryn R. Ayscough. 2009. "Differential Requirements for Actin during Yeast and Mammalian Endocytosis." *Nature Cell Biology* 11 (8): 1039–42. https://doi.org/10.1038/ncb1918.

Avasthi, Prachee, Masayuki Onishi, Joel Karpiak, Ryosuke Yamamoto, Luke Mackinder, Martin C Jonikas, Winfield S Sale, Brian Shoichet, John R Pringle, and Wallace F Marshall. 2014. "Actin Is Required for IFT Regulation in Chlamydomonas Reinhardtii." *Current Biology* 24 (17): 2025–32. https://doi.org/10.1016/j.cub.2014.07.038.

Ayscough, K. R., J. Stryker, N. Pokala, M. Sanders, P. Crews, and D. G. Drubin. 1997. "High Rates of Actin Filament Turnover in Budding Yeast and Roles for Actin in Establishment and Maintenance of Cell Polarity Revealed Using the Actin Inhibitor Latrunculin-A." *The Journal of Cell Biology* 137 (2): 399–416. https://doi.org/10.1083/jcb.137.2.399.

Basu, Roshni, Emilia Laura Munteanu, and Fred Chang. 2014. "Role of Turgor Pressure in Endocytosis in Fission Yeast." *Molecular Biology of the Cell* 25 (5): 679–87. https://doi.org/10.1091/mbc.E13-10-0618.

Belzile, Olivier, Carmen I Hernandez-Lara, Qian Wang, and William J Snell. 2013. "Regulated Membrane Protein Entry into Flagella Is Facilitated by Cytoplasmic Microtubules and Does Not Require IFT." *Current Biology : CB* 23 (15): 1460–65. https://doi.org/10.1016/j.cub.2013.06.025.

Bouck, G. Benjamin. 1971. "THE STRUCTURE, ORIGIN, ISOLATION, AND COMPOSITION OF THE TUBULAR MASTIGONEMES OF THE OCHROMONAS FLAGELLUM." *Journal of Cell Biology* 50 (2): 362–84. https://doi.org/10.1083/jcb.50.2.362.

Campellone, K., and M. Welch. 2010. "A Nucleator Arms Race: Cellular Control of Actin Assembly." *Nature Reviews Molecular Cell Biology* 11: 237–51.

841 Carlsson, Anders E., and Philip V. Bayly. 2014. “Force Generation by Endocytic Actin Patches in
842 Budding Yeast.” *Biophysical Journal* 106 (8): 1596–1606.
843 https://doi.org/10.1016/j.bpj.2014.02.035.
844 Cheng, Xi, Gai Liu, Wenting Ke, Lijuan Zhao, Bo Lv, Xiaocui Ma, Nannan Xu, et al. 2017. “Building
845 a Multipurpose Insertional Mutant Library for Forward and Reverse Genetics in
846 Chlamydomonas.” *Plant Methods* 13 (1): 36. https://doi.org/10.1186/s13007-017-0183-
847 5.
848 Cochilla, Amanda J., Joseph K. Angleson, and William J. Betz. 1999. “MONITORING SECRETORY
849 MEMBRANE WITH FM1-43 FLUORESCENCE.” *Annual Review of Neuroscience* 22 (1): 1–
850 10. https://doi.org/10.1146/annurev.neuro.22.1.1.
851 Craig, Evan W., David M. Mueller, Brae M. Bigge, Miroslava Schaffer, Benjamin D. Engel, and
852 Prachee Avasthi. 2019. “The Elusive Actin Cytoskeleton of a Green Alga Expressing Both
853 Conventional and Divergent Actins.” *Molecular Biology of the Cell*, mbc.E19-03-0141.
854 https://doi.org/10.1091/mbc.E19-03-0141.
855 Dentler, W L, and C Adams. 1992. “Flagellar Microtubule Dynamics in Chlamydomonas:
856 Cytochalasin D Induces Periods of Microtubule Shortening and Elongation; and
857 Colchicine Induces Disassembly of the Distal, but Not Proximal, Half of the Flagellum.”
858 *The Journal of Cell Biology* 117 (6): 1289–98. https://doi.org/10.1083/jcb.117.6.1289.
859 Dentler, William. 2013. “A Role for the Membrane in Regulating Chlamydomonas Flagellar
860 Length.” *PLOS ONE* 8 (1): e53366. https://doi.org/10.1371/journal.pone.0053366.
861 Diener, Dennis R, Pietro Lupetti, and Joel L Rosenbaum. 2015. “Proteomic Analysis of Isolated
862 Ciliary Transition Zones Reveals the Presence of ESCRT Proteins.” *Current Biology : CB* 25
863 (3): 379–84. https://doi.org/10.1016/j.cub.2014.11.066.
864 Farina, Francesca, Jérémie Gaillard, Christophe Guérin, Yohann Couté, James Sillibourne,
865 Laurent Blanchoin, and Manuel Théry. 2016. “The Centrosome Is an Actin-Organizing
866 Centre.” *Nature Cell Biology* 18 (1): 65–75. https://doi.org/10.1038/ncb3285.
867 Gachet, Yannick, and Jeremy S. Hyams. 2005. “Endocytosis in Fission Yeast Is Spatially
868 Associated with the Actin Cytoskeleton during Polarised Cell Growth and Cytokinesis.”
869 *Journal of Cell Science* 118 (Pt 18): 4231–42. https://doi.org/10.1242/jcs.02530.
870 Goode, Bruce L, Julian A Eskin, and Beverly Wendland. 2015. “Actin and Endocytosis in Budding
871 Yeast.” *Genetics* 199 (2): 315–58. https://doi.org/10.1534/genetics.112.145540.
872 Gournier, Helene, Erin D. Goley, Hanspeter Niederstrasser, Thong Trinh, and Matthew D.
873 Welch. 2001. “Reconstitution of Human Arp2/3 Complex Reveals Critical Roles of
874 Individual Subunits in Complex Structure and Activity.” *Molecular Cell* 8 (5): 1041–52.
875 https://doi.org/10.1016/S1097-2765(01)00393-8.
876 Hetrick, Byron, Min Suk Han, Luke A Helgeson, and Brad J Nolen. 2013. “Small Molecules CK-666
877 and CK-869 Inhibit Actin-Related Protein 2/3 Complex by Blocking an Activating
878 Conformational Change.” *Chemistry & Biology* 20 (5): 701–12.
879 https://doi.org/10.1016/j.chembiol.2013.03.019.
880 Hirono, Masafumi, Satomi Uryu, Akio Ohara, Takako Kato-Minoura, and Ritsu Kamiya. 2003.
881 “Expression of Conventional and Unconventional Actins in Chlamydomonas Reinhardtii
882 upon Deflagellation and Sexual Adhesion.” *Eukaryotic Cell* 2 (3): 486–93.
883 https://doi.org/10.1128/ec.2.3.486-493.2003.

884 Hu Qicong, Milenkovic Ljiljana, Jin Hua, Scott Matthew P., Nachury Maxence V., Spiliotis Elias T.,
885 and Nelson W. James. 2010. “A Septin Diffusion Barrier at the Base of the Primary Cilium
886 Maintains Ciliary Membrane Protein Distribution.” *Science* 329 (5990): 436–39.
887 https://doi.org/10.1126/science.1191054.
888 Inoue, Daisuke, Dorian Obino, Judith Pineau, Francesca Farina, Jérémie Gaillard, Christophe
889 Guerin, Laurent Blanchoin, Ana-Maria Lennon-Duménil, and Manuel Théry. 2019. “Actin
890 Filaments Regulate Microtubule Growth at the Centrosome.” *The EMBO Journal* 38 (11).
891 https://doi.org/10.15252/embj.201899630.
892 Jack, Brittany, and Prachee Avasthi. 2018. “Erratum to: Chemical Screening for Flagella-
893 Associated Phenotypes in Chlamydomonas Reinhardtii.” *Methods in Molecular Biology*
894 *(Clifton, N.J.)* 1795: E1. https://doi.org/10.1007/978-1-4939-7874-8_19.
895 Jack, Brittany, David M. Mueller, Ann C. Fee, Ashley L. Tetlow, and Prachee Avasthi. 2019.
896 “Partially Redundant Actin Genes in Chlamydomonas Control Transition Zone
897 Organization and Flagellum-Directed Traffic.” *Cell Reports* 27 (8): 2459-2467.e3.
898 https://doi.org/10.1016/j.celrep.2019.04.087.
899 Jin, Hua, Susan Roehl White, Toshinobu Shida, Stefan Schulz, Mike Aguiar, Steven P. Gygi, J.
900 Fernando Bazan, and Maxence V. Nachury. 2010. “The Conserved Bardet-Biedl
901 Syndrome Proteins Assemble a Coat That Traffics Membrane Proteins to Cilia.” *Cell* 141
902 (7): 1208–19. https://doi.org/10.1016/j.cell.2010.05.015.
903 Kaplan, Oktay I., David B. Doroquez, Sebiha Cevik, Rachel V. Bowie, Lara Clarke, Anna A.W.M.
904 Sanders, Katarzyna Kida, Joshua Z. Rappoport, Piali Sengupta, and Oliver E. Blacque.
905 2012. “Endocytosis Genes Facilitate Protein and Membrane Transport in C. Elegans
906 Sensory Cilia.” *Current Biology* 22 (6): 451–60.
907 https://doi.org/10.1016/j.cub.2012.01.060.
908 Kato-Minoura, T, S Uryu, M Hirono, and R Kamiya. 1998. “Highly Divergent Actin Expressed in a
909 Chlamydomonas Mutant Lacking the Conventional Actin Gene.” *Biochemical and*
910 *Biophysical Research Communications* 251 (1): 71–76.
911 https://doi.org/10.1006/bbrc.1998.9373.
912 Kiesel, Petra, Gonzalo Alvarez Viar, Nikolai Tsoy, Riccardo Maraspini, Peter Gorilak, Vladimir
913 Varga, Alf Honigmann, and Gaia Pigino. 2020. “The Molecular Structure of Mammalian
914 Primary Cilia Revealed by Cryo-Electron Tomography.” *Nature Structural & Molecular*
915 *Biology*, September. https://doi.org/10.1038/s41594-020-0507-4.
916 Kim, Joon, Ji Eun Lee, Susanne Heynen-Genel, Eigo Suyama, Keiichiro Ono, Kiyoung Lee, Trey
917 Ideker, Pedro Aza-Blanc, and Joseph G. Gleeson. 2010. “Functional Genomic Screen for
918 Modulators of Ciliogenesis and Cilium Length.” *Nature* 464 (7291): 1048–51.
919 https://doi.org/10.1038/nature08895.
920 Langousis, Gerasimos, Michelle M. Shimogawa, Edwin A. Saada, Ajay A. Vashisht, Roberto
921 Spreafico, Andrew R. Nager, William D. Barshop, Maxence V. Nachury, James A.
922 Wohlschlegel, and Kent L. Hill. 2016. “Loss of the BBSome Perturbs Endocytic Trafficking
923 and Disrupts Virulence of Trypanosoma Brucei.” *Proceedings of the National Academy*
924 *of Sciences of the United States of America* 113 (3): 632–37.
925 https://doi.org/10.1073/pnas.1518079113.
926 Lefebvre, P. A., S. A. Nordstrom, J. E. Moulder, and J. L. Rosenbaum. 1978. “Flagellar Elongation
927 and Shortening in Chlamydomonas. IV. Effects of Flagellar Detachment, Regeneration,

928 and Resorption on the Induction of Flagellar Protein Synthesis." *The Journal of Cell*
929 *Biology* 78 (1): 8–27. https://doi.org/10.1083/jcb.78.1.8.
930 Lefebvre, Paul A. 1995. "Flagellar Amputation and Regeneration in Chlamydomonas." In
931 *Methods in Cell Biology*, 47:3–7. Elsevier.
932 Li, Xiaobo, Weronika Patena, Friedrich Fauser, Robert E. Jinkerson, Shai Saroussi, Moritz T.
933 Meyer, Nina Ivanova, et al. 2019. "A Genome-Wide Algal Mutant Library and Functional
934 Screen Identifies Genes Required for Eukaryotic Photosynthesis." *Nature Genetics* 51
935 (4): 627–35. https://doi.org/10.1038/s41588-019-0370-6.
936 Loeffelholz, Ottilie von, Andrew Purkiss, Luyan Cao, Svend Kjaer, Naoko Kogata, Guillaume
937 Romet-Lemonne, Michael Way, and Carolyn A. Moores. 2020. "Cryo-EM of Human
938 Arp2/3 Complexes Provides Structural Insights into Actin Nucleation Modulation by
939 ARPC5 Isoforms." *BioRxiv*, January, 2020.05.01.071704.
940 https://doi.org/10.1101/2020.05.01.071704.
941 Lord, Samuel J., Katrina B. Velle, R. Dyche Mullins, and Lillian K. Fritz-Laylin. 2020. "SuperPlots:
942 Communicating Reproducibility and Variability in Cell Biology." *The Journal of Cell*
943 *Biology* 219 (6). https://doi.org/10.1083/jcb.202001064.
944 Macia, Eric, Marcelo Ehrlich, Ramiro Massol, Emmanuel Boucrot, Christian Brunner, and Tomas
945 Kirchhausen. 2006. "Dynasore, a Cell-Permeable Inhibitor of Dynamin." *Developmental*
946 *Cell* 10 (6): 839–50. https://doi.org/10.1016/j.devcel.2006.04.002.
947 Milenkovic, Ljiljana, Matthew P. Scott, and Rajat Rohatgi. 2009. "Lateral Transport of
948 Smoothened from the Plasma Membrane to the Membrane of the Cilium." *The Journal*
949 *of Cell Biology* 187 (3): 365–74. https://doi.org/10.1083/jcb.200907126.
950 Molla-Herman, Anahi, Rania Ghossoub, Thierry Blisnick, Alice Meunier, Catherine Serres, Flora
951 Silbermann, Chris Emmerson, et al. 2010. "The Ciliary Pocket: An Endocytic Membrane
952 Domain at the Base of Primary and Motile Cilia." *Journal of Cell Science* 123 (Pt 10):
953 1785–95. https://doi.org/10.1242/jcs.059519.
954 Monis, William J., Victor Faundez, and Gregory J. Pazour. 2017. "BLOC-1 Is Required for
955 Selective Membrane Protein Trafficking from Endosomes to Primary Cilia." *The Journal*
956 *of Cell Biology* 216 (7): 2131–50. https://doi.org/10.1083/jcb.201611138.
957 Nachury, Maxence V., Alexander V. Loktev, Qihong Zhang, Christopher J. Westlake, Johan
958 Peränen, Andreas Merdes, Diane C. Slusarski, et al. 2007. "A Core Complex of BBS
959 Proteins Cooperates with the GTPase Rab8 to Promote Ciliary Membrane Biogenesis."
960 *Cell* 129 (6): 1201–13. https://doi.org/10.1016/j.cell.2007.03.053.
961 Nachury, Maxence V., E. Scott Seeley, and Hua Jin. 2010. "Trafficking to the Ciliary Membrane:
962 How to Get across the Periciliary Diffusion Barrier?" *Annual Review of Cell and*
963 *Developmental Biology* 26: 59–87.
964 https://doi.org/10.1146/annurev.cellbio.042308.113337.
965 Nolen, Brad J., Ryan S. Littlefield, and Thomas D. Pollard. 2004. "Crystal Structures of Actin-
966 Related Protein 2/3 Complex with Bound ATP or ADP." *Proceedings of the National*
967 *Academy of Sciences of the United States of America* 101 (44): 15627.
968 https://doi.org/10.1073/pnas.0407149101.
969 Onishi, M., K. Pecani, T. th Jones, J. R. Pringle, and F. R. Cross. 2018. "F-Actin Homeostasis
970 through Transcriptional Regulation and Proteasome-Mediated Proteolysis." *Proc Natl*
971 *Acad Sci U S A* 115 (28): E6487-e6496. https://doi.org/10.1073/pnas.1721935115.

Onishi, M., J. R. Pringle, and F. R. Cross. 2016. “Evidence That an Unconventional Actin Can Provide Essential F-Actin Function and That a Surveillance System Monitors F-Actin Integrity in Chlamydomonas.” *Genetics* 202 (3): 977–96. https://doi.org/10.1534/genetics.115.184663.

Onishi, Masayuki, James G. Umen, Frederick R. Cross, and John R. Pringle. 2019. “Cleavage-Furrow Formation without F-Actin in Chlamydomonas</Em>.” *BioRxiv*, January, 789016. https://doi.org/10.1101/789016.

Papermaster, D. S., B. G. Schneider, and J. C. Besharse. 1985. “Vesicular Transport of Newly Synthesized Opsin from the Golgi Apparatus toward the Rod Outer Segment. Ultrastructural Immunocytochemical and Autoradiographic Evidence in Xenopus Retinas.” *Investigative Ophthalmology & Visual Science* 26 (10): 1386–1404.

Park, Tae Joo, Brian J. Mitchell, Philip B. Abitua, Chris Kintner, and John B. Wallingford. 2008. “Dishevelled Controls Apical Docking and Planar Polarization of Basal Bodies in Ciliated Epithelial Cells.” *Nature Genetics* 40 (7): 871–79. https://doi.org/10.1038/ng.104.

Pasquale, S M, and U W Goodenough. 1987. “Cyclic AMP Functions as a Primary Sexual Signal in Gametes of Chlamydomonas Reinhardtii.” *The Journal of Cell Biology* 105 (5): 2279–92. https://doi.org/10.1083/jcb.105.5.2279.

Pedersen, Lotte B., and Joel L. Rosenbaum. 2008. “Intraflagellar Transport (IFT) Role in Ciliary Assembly, Resorption and Signalling.” *Current Topics in Developmental Biology* 85: 23–61. https://doi.org/10.1016/S0070-2153(08)00802-8.

Pettersen, Eric F., Thomas D. Goddard, Conrad C. Huang, Gregory S. Couch, Daniel M. Greenblatt, Elaine C. Meng, and Thomas E. Ferrin. 2004. “UCSF Chimera--a Visualization System for Exploratory Research and Analysis.” *Journal of Computational Chemistry* 25 (13): 1605–12. https://doi.org/10.1002/jcc.20084.

Ranjan, Peeyush, Mayanka Awasthi, and William J. Snell. 2019. “Transient Internalization and Microtubule-Dependent Trafficking of a Ciliary Signaling Receptor from the Plasma Membrane to the Cilium.” *Current Biology* 29 (17): 2942-2947.e2. https://doi.org/10.1016/j.cub.2019.07.022.

Robinson, Robert C., Kirsi Turbedsky, Donald A. Kaiser, Jean-Baptiste Marchand, Henry N. Higgs, Senyon Choe, and Thomas D. Pollard. 2001. “Crystal Structure of Arp2/3 Complex.” *Science* 294 (5547): 1679. https://doi.org/10.1126/science.1066333.

Rohatgi, Rajat, and William J Snell. 2010. “The Ciliary Membrane.” *Current Opinion in Cell Biology* 22 (4): 541–46. https://doi.org/10.1016/j.ceb.2010.03.010.

Rosenbaum, J. L., J. E. Moulder, and D. L. Ringo. 1969. “Flagellar Elongation and Shortening in Chlamydomonas. The Use of Cycloheximide and Colchicine to Study the Synthesis and Assembly of Flagellar Proteins.” *The Journal of Cell Biology* 41 (2): 600–619. https://doi.org/10.1083/jcb.41.2.600.

Saito, Masaki, Wataru Otsu, Kuo-Shun Hsu, Jen-Zen Chuang, Teruyuki Yanagisawa, Vincent Shieh, Taku Kaitsuka, Fan-Yan Wei, Kazuhito Tomizawa, and Ching-Hwa Sung. 2017. “Tctex-1 Controls Ciliary Resorption by Regulating Branched Actin Polymerization and Endocytosis.” *EMBO Reports* 18 (8): 1460–72. https://doi.org/10.15252/embr.201744204.

1014 Sali, A., and T. L. Blundell. 1993. “Comparative Protein Modelling by Satisfaction of Spatial
1015 Restraints.” *Journal of Molecular Biology* 234 (3): 779–815.
1016 https://doi.org/10.1006/jmbi.1993.1626.
1017 Spector, Ilan, Nava R. Shochet, Dina Blasberger, and Yoel Kashman. 1989. “Latrunculins—Novel
1018 Marine Macrolides That Disrupt Microfilament Organization and Affect Cell Growth: I.
1019 Comparison with Cytochalasin D.” *Cell Motility* 13 (3): 127–44.
1020 https://doi.org/10.1002/cm.970130302.
1021 Willox, Anna K., Yasmina M. E. Sahraoui, and Stephen J. Royle. 2014. “Non-Specificity of Pitstop
1022 2 in Clathrin-Mediated Endocytosis.” *Biology Open* 3 (5): 326–31.
1023 https://doi.org/10.1242/bio.20147955.
1024 Wingfield, Jenna L, Ilaria Mengoni, Heather Bomberger, Yu-Yang Jiang, Jonathon D Walsh, Jason
1025 M Brown, Tyler Picariello, et al. 2017. “IFT Trains in Different Stages of Assembly Queue
1026 at the Ciliary Base for Consecutive Release into the Cilium.” Edited by Erwin J G
1027 Peterman. *ELife* 6 (May): e26609. https://doi.org/10.7554/eLife.26609.
1028 Winter, D. C., E. Y. Choe, and R. Li. 1999. “Genetic Dissection of the Budding Yeast Arp2/3
1029 Complex: A Comparison of the in Vivo and Structural Roles of Individual Subunits.”
1030 *Proceedings of the National Academy of Sciences of the United States of America* 96
1031 (13): 7288–93. https://doi.org/10.1073/pnas.96.13.7288.
1032 Wood, Christopher R., and Joel L. Rosenbaum. 2014. “Proteins of the Ciliary Axoneme Are
1033 Found on Cytoplasmic Membrane Vesicles during Growth of Cilia.” *Current Biology* 24
1034 (10): 1114–20. https://doi.org/10.1016/j.cub.2014.03.047.
1035 Wu, Chien-Ting, Hsin-Yi Chen, and Tang K. Tang. 2018. “Myosin-Va Is Required for Preciliary
1036 Vesicle Transportation to the Mother Centriole during Ciliogenesis.” *Nature Cell Biology*
1037 20 (2): 175–85. https://doi.org/10.1038/s41556-017-0018-7.
1038 Zuo, Xiaofeng, Wei Guo, and Joshua H. Lipschutz. 2009. “The Exocyst Protein Sec10 Is Necessary
1039 for Primary Ciliogenesis and Cystogenesis In Vitro.” *Molecular Biology of the Cell* 20 (10):
1040 2522–29. https://doi.org/10.1091/mbc.e08-07-0772.
1041
1042